

Record Number: 14050
Author, Monographic: Morin, J.//Lafleur, J.//Côté, S.//Boudreau, P.//Leclerc, M.
Author Role:
Title, Monographic: Integrated hydrodynamic, waves and plants habitat modeling for restoration of shoreline on Clark island, lake St. Francis
Translated Title:
Reprint Status:
Edition:
Author, Subsidiary:
Author Role:
Place of Publication: Québec
Publisher Name: INRS-Eau
Date of Publication: 1997
Original Publication Date: Juillet 1997
Volume Identification:
Extent of Work: vii, 48
Packaging Method: pages
Series Editor:
Series Editor Role:
Series Title: INRS-Eau, rapport de recherche
Series Volume ID: 503
Location/URL:
ISBN: 2-89146-469-9
Notes: Rapport annuel 1997-1998
Abstract: Rapport préparé pour Tecsalt Environment Inc.
Call Number: R000503
Keywords: rapport/ ok/ dl

**Integrated hydrodynamic, waves and plant
habitat modeling for shoreline restoration
on Clark Island, Lake St. Francis**

**Integrated hydrodynamic, waves and plant habitat modeling
for shoreline restoration on Clark Island, Lake St. Francis**

**report prepared for :
Tecsult Environment Inc.**

INRS-Eau, rapport de recherche no 503

July 1997

INRS-EAU SCIENTIFIC TEAM

Project Director Michel Leclerc, M.Sc., Dr. Ing., Professor-researcher

Project Manager Jean Morin, M.Sc., Ph.D. student

Specialists Julie Lafleur, M.Sc. research agent

Paul Boudreau, M.Sc., research agent

Steve Côté, M.Sc. student

TECSULT TEAM

Project Manager Roméo Ciobotariu,

Project Engineer Marie-Claude Wilson,

Hydraulic specialist Gaétan Thibault,

We thank Ronald Greendale for reviewing the manuscript.

To be cited as :

Morin, J., Lafleur, J., Côté, S., Boudreau, P., Leclerc, M., 1997. Integrated hydrodynamic, waves and plants habitat modeling for restoration of shoreline on Clark Island, Lake St. Francis. For Tecsult Environment Inc. INRS-EAU research report # 503

Table of contents

1. Introduction	1
2. Hydrodynamic modeling	3
2.1. Data.....	3
2.1.1. Topography.....	3
2.1.2. Aquatic plants	4
2.1.3. Substrate	4
2.1.4. Hydrology.....	4
2.2. Modeling the hydrodynamics.....	6
2.2.1. Hydrodynamic model	6
2.2.2. Discretization	7
2.2.3. Initial and boundary conditions.....	9
2.2.4. Calibration and validation.....	9
2.2.5. Integrating the capping structure.....	14
2.3. Results of hydrodynamic modeling	16
2.3.1. Reference state : 8200 m ³ /s.....	16
2.3.2. Average summer flow : 7 800 m ³ /s.....	18
2.3.3. Minimum summer flow : 6 500 m ³ /s	19
2.3.4. Maximum flow : 9 622 m ³ /s, with the capping structure	21
2.3.5. Maximum flow : 9 622 m ³ /s, without the capping structure	23
2.3.6. Impact of the capping structure	25
3. Wave modeling.....	27
3.1. Data.....	27
3.1.1. Topography.....	27
3.1.2. Wind statistics and choice of event	27
3.2. Modeling the waves.....	27
3.2.1. Wave model HISWA	27
3.2.2. Discretization	28
3.2.3. Initial and boundary conditions.....	28
3.3. Results of wave modeling	28
3.3.1. Without the capping structure	29
3.3.2. Ground-truthing observations.....	29
3.3.3. With the capping structure	29

4. Plants habitat	31
4.1. Methodology of plants analysis	31
4.2. Field observations and habitat	31
4.2.1. Description of abiotic factors	33
4.3. Choice of plants for revegetalization	34
4.4. Habitat characteristics the capping structure	34
5. Analysis of the new capping structure	35
5.1. Modification of the capping structure design	35
5.1.1. Description of the new design	35
5.1.2. Main advantages of the new design	36
5.2. Hydrodynamic modeling	36
5.2.1. Data	36
5.2.2. Modeling the hydrodynamics.....	37
5.2.3. Results of hydrodynamic modeling.....	37
5.3. Wave modeling	40
5.3.1. Data	40
5.3.2. Modeling the waves	40
5.3.3. Result of wave modeling	40
5.4. Plant habitat modeling	42
5.4.1. Methodology	42
5.4.2. Recommendation for revegetalization	42
5.4.3. Recommendations for structure amelioration	42
6. Conclusions	45
7. References	46

List of figures

Figure 1 : Main steps of the methodology.	2
Figure 2 : Boundaries of the flow domain.	3
Figure 3 : Six node element used in the discretization.	7
Figure 4 : Finite element grid of the flow domain.	8
Figure 5 : Finite element grid in the vicinity of Clark Island.	8
Figure 6 : Validation results for velocity measurements.	12
Figure 7 : Depth in the vicinity of Clark Island for the validation of the reference state.	13
Figure 8 : Velocity in the vicinity of Clark Island for the validation of the reference state.	13
Figure 9 : Illustration of the capping structure.	14
Figure 10 : Profile of the capping structure.	14
Figure 11 : Actual topography of the northwest shoreline of Clark Island.	15
Figure 12 : Modified topography of the northwest shoreline of Clark Island taking into account the capping structure.	15
Figure 13 : Depth in the vicinity of Clark Island at a flow of 8 200 m ³ /s.	17
Figure 14 : Velocity in the vicinity of Clark Island at a flow of 8 200 m ³ /s.	17
Figure 15 : Depth in the vicinity of Clark Island at a flow of 7 800 m ³ /s.	18
Figure 16 : Velocity in the vicinity of Clark Island at a flow of 7 800 m ³ /s.	19
Figure 17 : Depth in the vicinity of Clark Island at a flow of 6 500 m ³ /s.	20
Figure 18 : Velocity in the vicinity of Clark Island at a flow of 6 500 m ³ /s.	20
Figure 19 : Depth in the vicinity of Clark Island at a flow of 9 622 m ³ /s with the capping structure.	21
Figure 20 : Velocity in the vicinity of Clark Island at a flow of 9 622 m ³ /s with the capping structure.	22
Figure 21 : Shear velocity in the vicinity of Clark Island at a flow of 9 622 m ³ /s with the capping structure.	22
Figure 22 : Depth in the vicinity of Clark Island at a flow of 9 622 m ³ /s without the capping structure.	23
Figure 23 : Velocity in the vicinity of Clark Island at a flow of 9 622 m ³ /s without the capping structure.	24
Figure 24 : Shear velocity in the vicinity of Clark Island at a flow of 9 622 m ³ /s without the capping structure.	24
Figure 25 : Differences between velocities simulated with and without the capping structure at a flow of 8200 m ³ /s.	25
Figure 26 : Wave induced shear velocities without the capping structure.	30
Figure 27 : Wave induced shear velocities with the capping structure.	30
Figure 28 : Field photos of island shore.	32
Figure 29 : Illustration of the new capping structure.	35
Figure 30 : Profile of the new capping structure.	36

Figure 31 : Depth in the vicinity of Clark Island at a flow of 8 200 m ³ /s with the new capping structure.	38
Figure 32 : Velocity in the vicinity of Clark Island at a flow of 8 200 m ³ /s with the new capping structure.	38
Figure 33 : Shear velocity in the vicinity of Clark Island at a flow of 8 200 m ³ /s with the new capping structure.	39
Figure 34 : Differences between velocities simulated with and without the new capping structure at a flow of 8200 m ³ /s.	39
Figure 35 : Water depth within the capping structure as introduced in the wave model (created with 8 200 m ³ /s simulation).	41
Figure 36: Wave induced shear velocities with the new capping structure.	41
Figure 37: Recommendation for revegetalization.	44
Figure 38: Recommendation for structure amelioration.	44

List of tables

Table 1 : Transited discharges for different hydrological events.....	5
Table 2 : Hydrological conditions for the validation reference state	9
Table 3 : Measured and calculated discharges for different sections	10
Table 4 : Validation results for velocity measurements.....	11
Table 5 : Water level calculated by the hydrodynamic model at different points of interest	26
Table 6 : Habitat preferences of selected species.....	33

1. Introduction

This study is part of the Clark Island sediment rehabilitation project. Clark Island is located at the outlet of Lake St. Francis, 1.5 km west of Valleyfield, Québec. The island is currently owned by General Chemical Canada Ltd. (GCCL) ; prior to 1986, it was owned by Allied Chemical, now AlliedSignal, who operated several industrial facilities on the island. In 1986, the *Ministère de l'environnement et de la faune du Québec* (MEF) requested that AlliedSignal characterize the impacted sediments around the island. Between 1987 and 1993, several sediments characterization studies were conducted by Tecsult. Zone A, located on the northwest shore of Clark Island, has been identified by MEF as the area requiring the most attention because it contains contaminated sediments, mostly pyrite cinders, resulting from AlliedSignal industrial activities. The proposed remediation solution for this zone consists in physically isolating the contaminated sediments with the help of an engineered cap.

Since currents appeared to be the main physical factor influencing the site, INRS-Eau was contracted to simulate the hydrodynamics around Clark Island in order to assess the effect of current velocities on the engineered cap and to propose adequate vegetation for the site. However, evidence of relatively important wave-induced erosion suggested that waves were also a control mechanism of substrate variations and plant species distribution. Therefore, INRS-Eau undertook modeling the waves at the site, both in the absence and the presence of the capping structure, in order to better predict future plant distribution and growth.

This report investigates the hydrodynamics, the waves and the emergent aquatic vegetation around Clark Island (Figure 1). Hydrodynamic simulations were produced for several flow discharge scenarios. Waves produced by exceptionally strong winds from several directions were simulated and their impacts on the capping structure and on plants were analyzed. A survey of local emergent aquatic plants was conducted and their abiotic preferences were determined. Modifications to the planned capping structure were proposed in order to produce a healthy, diversified and stable environment, and an analysis of a new design was performed.

Chapters 2, 3 and 4 of this report were built using the first design of the capping structure : following recommendations, the design was modified by Tecsult to what is called herein the « new design ». This new design is fully analyzed in Chapter 5. Chapter 2 presents the hydrodynamic simulations, Chapter 3 addresses the modeling and interpretation of wind wave, Chapter 3 analyses the abiotic needs of emergent plants and their distribution. Chapter 5 presents a modified capping structure (new design) which was analyzed for hydrodynamics, waves and plant colonization.

The main steps of the methodology used in the Clark Island study are described in figure 1.

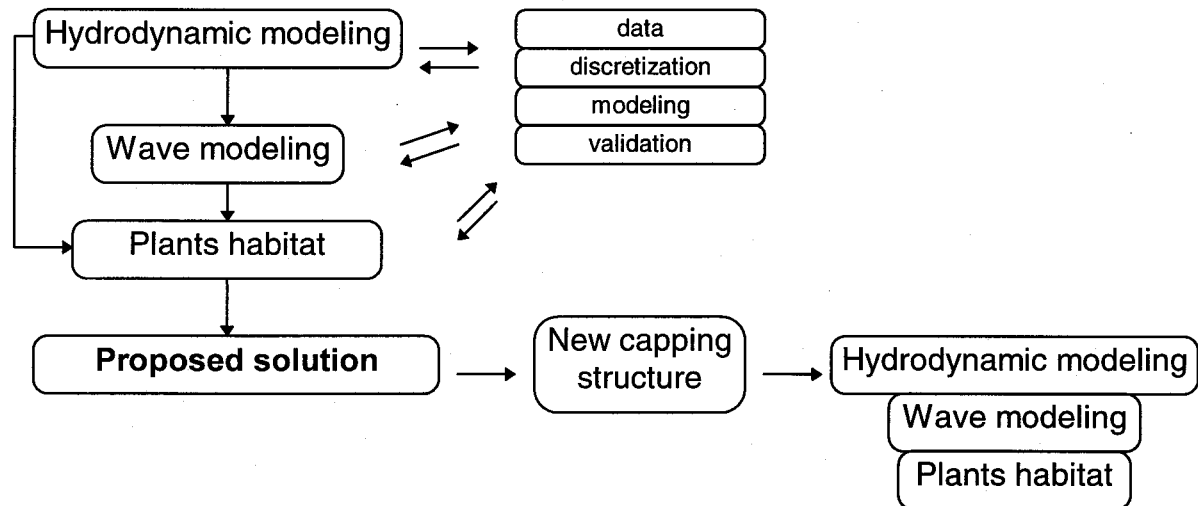


Figure 1 : Main steps of the methodology.

Three main topics were considered in order to define an optimized solution for the reintroduction of vegetation at the site. Hydrodynamics, waves and plant habitat are successively analyzed following the same procedure : data collection, discretization of the data, modeling and validation of the results. Only plant habitat assessment has a slightly different work sequence.

Most of the images of this report were produced with the MODELEUR (Secretan *et al.* 1996), a powerful G.I.S. built specifically for fluvial application. This tool has strong modeling capabilities and works with either triangular or regular rectangular elements for finite element applications, as well as for finite difference programs.

2. Hydrodynamic modeling

2.1. Data

The first step in hydrodynamics modeling is to collect two sets of physical data : a detailed topography of the river reach to be simulated with a description of riverbed materials and aquatic plants, and a reliable stage-discharge relationship at the downstream boundary of the river reach under study.

2.1.1. Topography

The topography of Lake St. Francis is well documented. Around 250 000 measurement points, available from the Canadian Hydrographic Service, cover the entire lake. Almost 100 000 of those points are located in the modeled reach of Lake St. Francis which runs from a transversal section located about 20 km upstream from Clark Island down to the inlet of the Beauharnois canal and to the Coteau hydraulic structures (see figure 2). A detailed topography around Clark Island has also been provided by Tecsult. The topography used for the hydrodynamic simulations is based on RIGL 55. Therefore, the data provided by Tecsult has been converted from RIGL 85 to RIGL 55 (8 cm lower than RIGL 85).

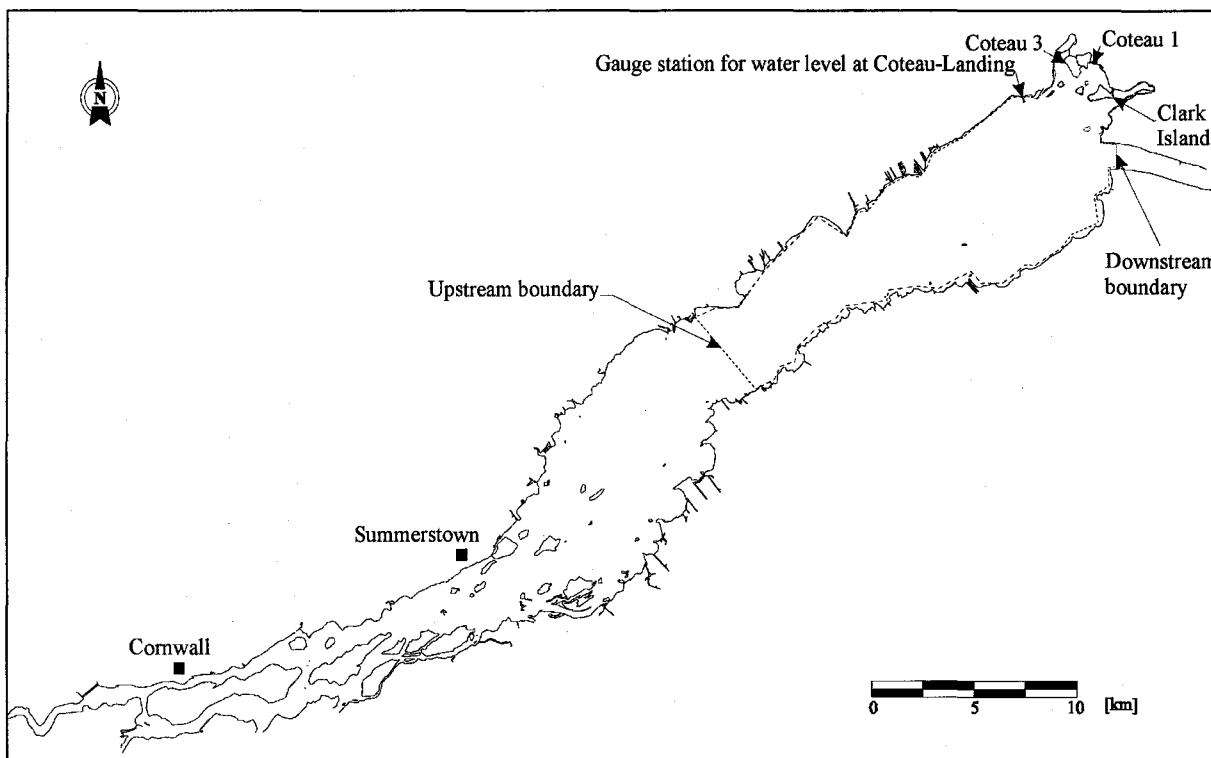


Figure 2 : Boundaries of the flow domain.

2.1.2. Aquatic plants

Submerged aquatic plants must be incorporated in the model for summer and early fall simulations because their occurrence creates significant friction affecting the flow pattern (Morin *et al* 1996). Seven species are considered abundant, forming 12 distinct vegetation systems distributed all over the lake bottom from very shallow depths to more than 12 m. For the hydrodynamic simulations, we used the plant distribution map and the related Manning's friction coefficient from Morin *et al.* (1996). This friction coefficient is calculated using a function that takes into account the state of annual growth, the relative composition of plant species, their size and their density. Manning's coefficient is then interpolated to the nodes of the finite element grid.

2.1.3. Substrate

Substrate, along with aquatic plants, creates friction along the bottom. Precise spatial distribution of various grain diameters is essential for hydrodynamic modeling. The substrate of Lake St. Francis has been mapped in detail by Morin and Leclerc (in prep) using precise topographic maps of the lake, 16 000 qualitative observation stations from the Canadian Hydrographic Service, 325 sampling stations with granulometric analyses available in the literature and 250 field observations. The map was then digitized and included in the model with the Manning's friction coefficient. For the purpose of the hydrodynamic simulation, Manning's coefficient « n » was calculated using a mean substrate diameter in accordance with the following equation (Morin and Leclerc, in prep) :

$$\frac{1}{n} = 34.9(-\log \bar{d}')^{0.31} \quad (1)$$

where,

\bar{d}' = average grain diameter (m).

The average grain diameter was calculated for each combination of materials with the following equation :

$$\bar{d}' = \sum_{i=1}^p w_i d_i \quad (2)$$

where,

d_i = median value of the i th class

w_i = weight used according to the number of substrate classes

p = number of classes identified at each observation point

2.1.4. Hydrology

The data on the hydrological regime of Lake St. Francis (Table 1) was derived from Morin *et al.* (1994). Lake St. Francis has a mean annual flow of 7 500 m³/s, of which more than 95% originates from Lake Ontario. The maximum monthly flow recorded between 1962 and 1993 is

10 012 m³/s (May 1993) and the minimum monthly flow recorded during the same period is 4 999 m³/s (May 1965). Most of the water in Lake St. Francis flows into Lake St. Louis through the Beauharnois canal where it is used for power generation. The portion of the flow discharge diverted to the Beauharnois canal is managed by the Coteau control structures ; a minimum flow of 290 m³/s must be evacuated through those structures at all times to maintain acceptable environmental conditions.

Since December 1993, Hydro-Québec applies the following policy in operating the Coteau control structures:

- The minimum flow at Coteau 3 between July 16th and April 14th is 200 m³/s ; from April 15th to July 15th it is 300 m³/s ;
- at Coteau 1, the minimum flow is 90 m³/s from July 16th to April 14th and 140 m³/s from April 15th to July 15th ;
- if the total discharge transiting through the Coteau control structures is less than 1 440 m³/s, the flow at Coteau 3 is kept at 200 m³/s or 300 m³/s, depending on the season, and the remaining water flows through Coteau 1 ;
- if the total discharge is more than 1 440 m³/s, all exceeding flow is split between Coteau 1 and Coteau 3.

The water level at Coteau-Landing is usually kept at around 46.42 m - RIGL 55 (RIGL 85 : 46.5) in summer and 46.48 m - RIGL 55 (RIGL 85 : 46.56) in winter. However, fluctuations occur (min. : 46.25 m and max. : 46.55 m). This data has been used as a reference to validate the water level of each hydrodynamic simulation.

Table 1 : Transited discharges for different hydrological events

Hydrological event	Transited discharges (m ³ /s)	
	Upstream boundary	Coteau control structures
Average summer flow (August)	7 800	1 000
Low summer flow (July)	6 500	500
Maximum flow (April)	9 622	4 533

2.2. Modeling the hydrodynamics

2.2.1. Hydrodynamic model

The hydrodynamic modeling was performed using the HYDROSIM model developed at INRS-Eau (see Heniche *et al.* 1997). The approach used is based on the two-dimensional numerical modeling of the shallow water equations, which are solved using the finite element method. It represents the mass and momentum conservation principles, and takes into account the local granulometric assemblage for the bottom friction parametrization. It produces reliable predictions of mean velocity, water level, and discharges for a wide range of hydrological conditions. The wetted surface is also solved by the model since it incorporates a drying-wetting capability allowing to estimate the flow boundary dynamically. The theoretical model is represented by the following system :

Mass conservation

$$\frac{\partial h}{\partial t} + \frac{\partial q_x}{\partial x} + \frac{\partial q_y}{\partial y} = 0 \quad (3)$$

Momentum conservation

$$\begin{aligned} \frac{\partial}{\partial x} \left(\frac{q_x q_x}{H} \right) + \frac{\partial}{\partial y} \left(\frac{q_x q_y}{H} \right) + c^2 \frac{\partial h}{\partial x} - \frac{1}{\rho} \left(\frac{\partial}{\partial x} (H \tau_{xx}) + \frac{\partial}{\partial y} (H \tau_{xy}) - \tau_x^b + \tau_x^s \right) - f_c q_y = 0 \\ \frac{\partial}{\partial x} \left(\frac{q_y q_x}{H} \right) + \frac{\partial}{\partial y} \left(\frac{q_y q_y}{H} \right) + c^2 \frac{\partial h}{\partial y} - \frac{1}{\rho} \left(\frac{\partial}{\partial x} (H \tau_{yx}) + \frac{\partial}{\partial y} (H \tau_{yy}) - \tau_y^b + \tau_y^s \right) + f_c q_x = 0 \end{aligned} \quad (4)$$

where,

$\mathbf{x}(x,y)$ = Cartesian components ;

t = time (s);

q_x, q_y = specific discharge with regard to x and y (m^2/s);

h = water surface level (m);

z_f = bed level with respect to a reference plane (m);

H = water depth ($=h-z_f$) (m);

c = celerity of waves ($c = \sqrt{gH}$) (m/s);

ρ = density of the water equal to 10^3 kg/m^3 ;

$\mathbf{u}(u,v)$ = velocity components which are given by the following relationship (m/s);

$u = q_x / H$ (m/s)

$v = q_y / H$ (m/s)

f_c = Coriolis factor ($f_c = 2\omega \sin\phi$) (s^{-1})

τ_{ij} = Reynolds stresses ($\text{kg/s}^2\text{m}$)

τ_x^b, τ_y^b = bottom friction in x and y directions ($\text{kg/s}^2\text{m}$)

τ_x^s, τ_y^s = surface stresses in x and y directions ($\text{kg/s}^2\text{m}$)

2.2.2. Discretization

The hydrodynamic model uses a discretization approach based on the finite elements method. The element is composed of six nodes, all involved (linear approximation on 4 triangular sub-elements) to predict the velocities (Figure 3). The geometry and water level only use the three corner nodes to provide a linear approximation of these variables. After discretization, mean velocity, water level and depth can be predicted at every node, or estimated at any point of the flow domain using numerical interpolation.

It involves the subdivision of the flow domain in a number of triangular elements, which size and shape can be adapted to represent the topographic and substrate variations as closely as possible. The grid is generated automatically with MODELEUR (Secretan *et al.* 1996). The resulting grid, which supports all the information related to topography, substrate and aquatic plants, is known as the numerical field model (NFM). The grid for the study area in Lake St. Francis comprises 12 217 elements and 25 137 nodes. Figure 4 and 5 present the finite element grid of the modeled reach. A finer grid was constructed for the main channel and for the close vicinity of Clark Island to better represent topographic variations. The mesh size varies from 10 meters in the vicinity of Clark Island to 400 meters in the shallow areas upstream from Clark Island.

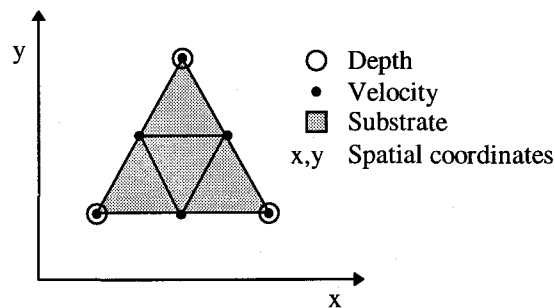


Figure 3 : Six node element used in the discretization.

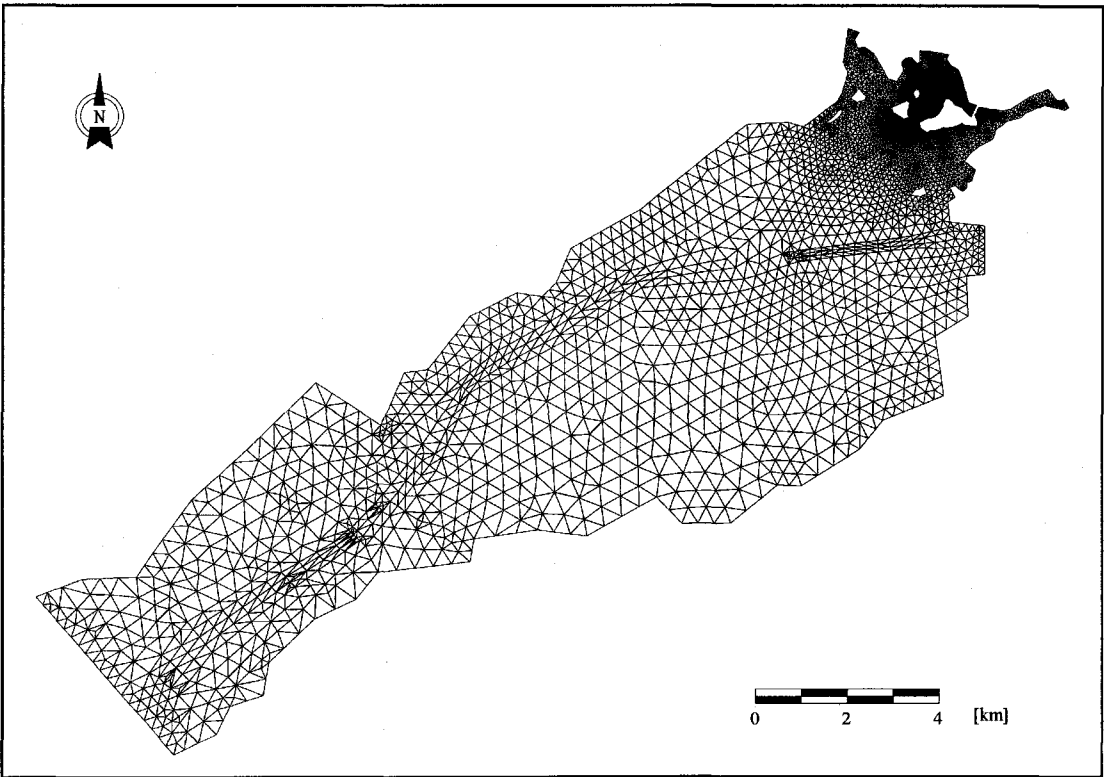


Figure 4 : Finite element grid of the flow domain.

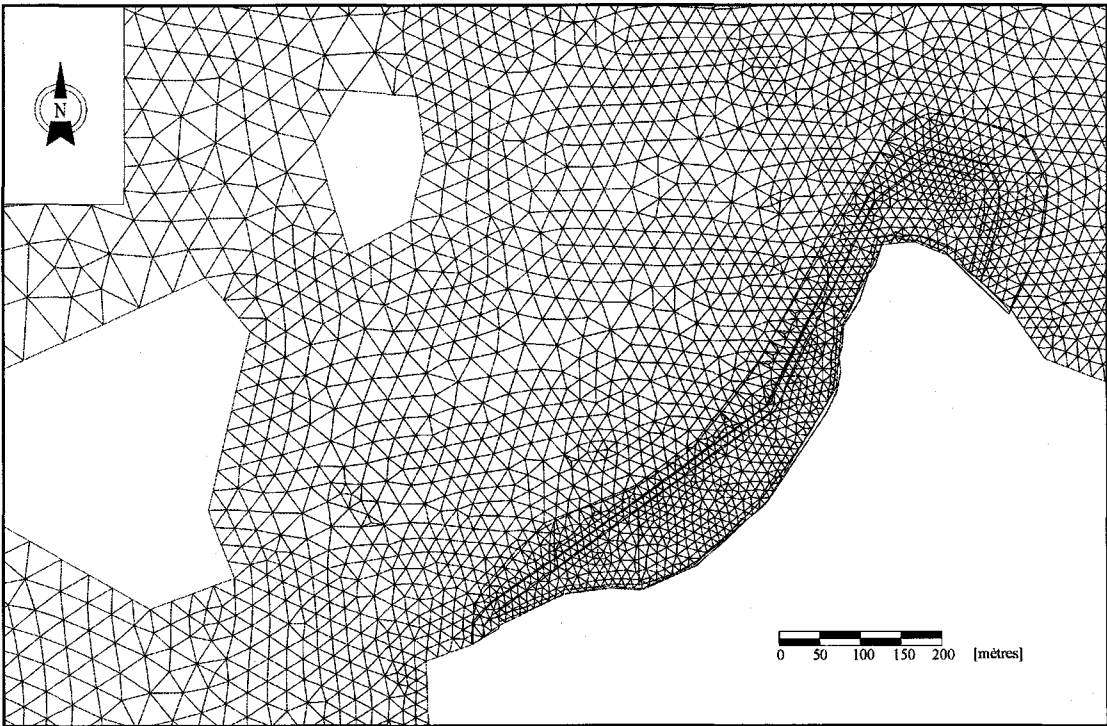


Figure 5 : Finite element grid in the vicinity of Clark Island.

2.2.3. Initial and boundary conditions

In this study, steady state conditions were simulated, which did not require special attention to the initial conditions. This implies that the final result for a particular state is independent of the initial conditions. However, the simulation must be sufficiently long to eliminate the errors associated with estimated initial conditions. Either the initial conditions were chosen from the closest hydrological conditions already simulated, or a uniform water level, corresponding to the average water level of the flow domain at the discharge considered, was specified.

Boundary conditions can be given as a global discharge, water level or distributed specific discharge. The closed lateral river boundaries were specified as having null tangential and normal velocities. The total river discharge was specified at the upstream boundary and the discharges at the Coteau control structures 1 and 3 were stated as downstream boundary conditions for each simulation. The water level was specified at the Beauharnois canal.

2.2.4. Calibration and validation

Calibration consists essentially in adjusting the value of the flow resistance parameters, i.e. the Manning's bottom friction coefficient n , and the turbulent viscosity ν_t . Since the Manning's n value was calculated with an already calibrated relationship (equation 1), there were only slight adjustments to be made. For this study, a constant turbulent viscosity of $15 \text{ m}^2/\text{s}$ was retained.

The validation reference state corresponds to the event of October 1st and October 2nd 1996, on which days some velocity measurements ($N=36$) were taken by Tecsult. The river hydrological conditions on both days along with the values used as boundary conditions for the validation simulation are presented in Table 2.

Table 2 : Hydrological conditions for the validation reference state

Variable	Event considered		
	October 1 st	October 2 nd	Validation
Discharge at the upstream boundary	n/d	8 300 m ³ /s	8 200
Discharge at Coteau 1 control structure	351 m ³ /s	428 m ³ /s	350
Discharge at Coteau 3 control structure	200 m ³ /s	200 m ³ /s	200
Water level at Beauharnois canal (m) ⁽¹⁾	n/d	n/d	46.36 (46.44)
Water level at Coteau-Landing (m) ⁽¹⁾	46.42(46.50)	46.42(46.50)	46.42 (46.50)

⁽¹⁾The value in parentheses correspond to a RIGL 85 reference whereas all other water level given in this table are based on RIGL 55. The difference between the two values is 8 cm.

Since discharges had been measured for a few sections on October 1st and 2nd, this data was also used to validate the hydrodynamic model. The comparison between measured and calculated discharges is presented in table 3. The errors observed are small and negligible, having no significant influence on the depth and the velocities simulated near the capping structure.

Table 3 : Measured and calculated discharges for different sections

Points of water passage	Specified or measured discharge (m ³ /s)	Calculated discharge (m ³ /s)	% difference between discharges
Upstream boundary	8 200	8 166	< 1
Coteau 1 control structure	350	330	6
Coteau 3 control structure	200	184	8
Beauharnois canal	7 650	7 609	< 1
Section 1 ⁽¹⁾	160	170	6

⁽¹⁾Location of sections is given in figure 6.

Differences between measured and calculated velocities were established for all measures available (Table 4). Overall, 78% of the velocity predictions were within 0.05 m/s of measured values. In this particular case, the precision of the current meter is not known ; however it is usually around 0.03 m/s. Greater differences in section 1 may be attributed to the fact that the bridge, close to which all measurements for this section were made, was not explicitly considered in the hydrodynamic simulations. Indeed, bridge piles may be responsible for local current phenomena. Figure 6 illustrates the velocity measurements taken by Tecsult compared with the calculated velocities. The orientation given to the measured velocities was based on the orientation of the calculated velocities for each measurement, since directions of the measured velocities were not available. Figure 7 and 8 show the depth and the velocity pattern for the validation reference state.

Table 4 : Validation results for velocity measurements.

	No ⁽¹⁾	Velocity (m/s)		Differences
		Measured	Calculated	
Section 1	1	0.130	0.074	-0.056
	2	0.130	0.114	-0.016
	3	0.150	0.156	0.006
	4	0.130	0.159	0.029
	5	0.200	0.164	-0.036
	6	0.160	0.167	0.007
	7	0.140	0.174	0.034
	8	0.160	0.180	0.020
	9	0.110	0.181	0.071
	10	0.200	0.182	-0.018
	11	0.170	0.182	0.012
	12	0.120	0.178	0.058
	13	0.120	0.164	0.044
	14	0.000	0.161	0.161
	15	0.110	0.154	0.044
	16	0.080	0.150	0.070
	17	0.050	0.127	0.077
	18	0.020	0.097	0.077
Section 2	1	0.120	0.112	-0.008
	2	0.170	0.112	-0.058
	3	0.030	0.066	0.036
	4	0.020	0.064	0.044
	5	0.040	0.057	0.017
Section 3	1	0.040	0.015	-0.025
	2	0.030	0.019	-0.011
	3	0.000	0.011	0.011
Section 4	1	0.110	0.085	-0.025
	2	0.090	0.099	0.009
	3	0.100	0.092	-0.008
	4	0.140	0.089	-0.051
	5	0.020	0.028	0.008
Section 5	1	0.040	0.022	-0.018
	2	0.040	0.014	-0.026
	3	0.050	0.020	-0.030
	4	0.050	0.015	-0.035
	5	0.020	0.024	0.004

⁽¹⁾ Refer to figure 5.7 of chapter 5 in Clark Island Site - Environmental Impact Study.

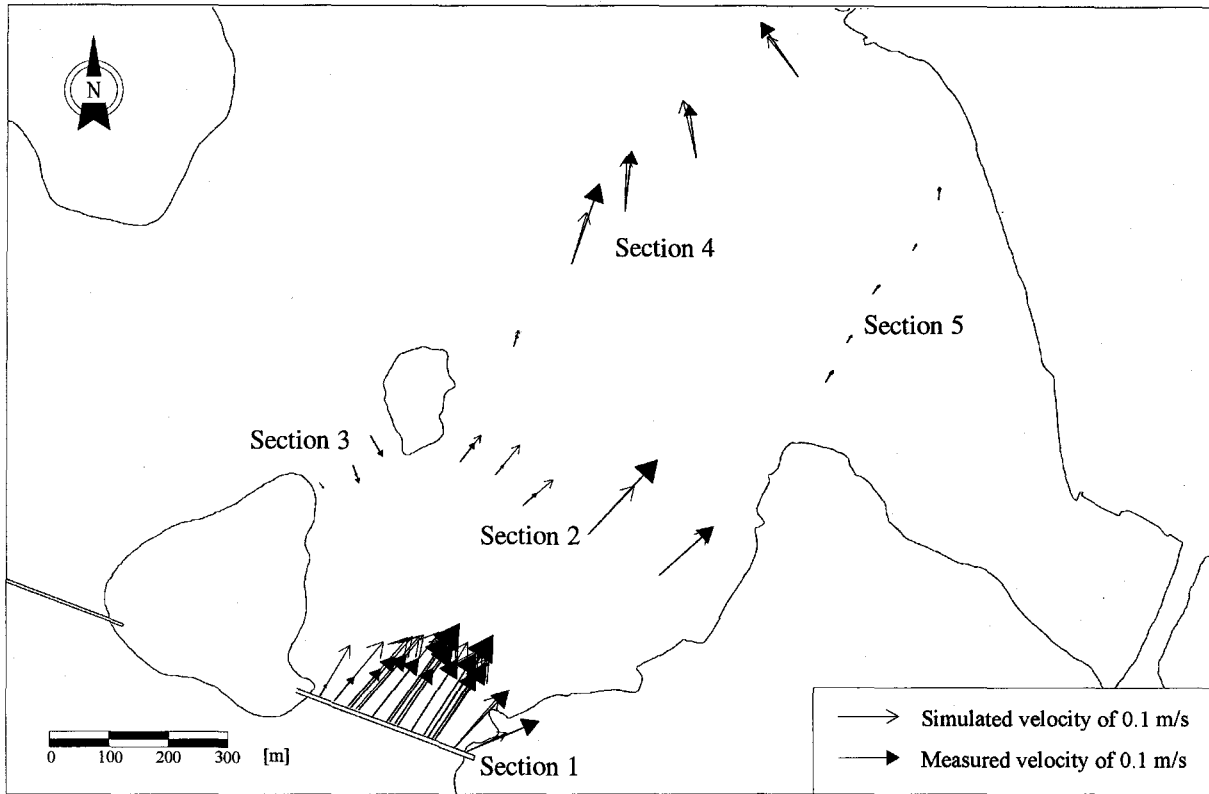


Figure 6 : Validation results for velocity measurements.

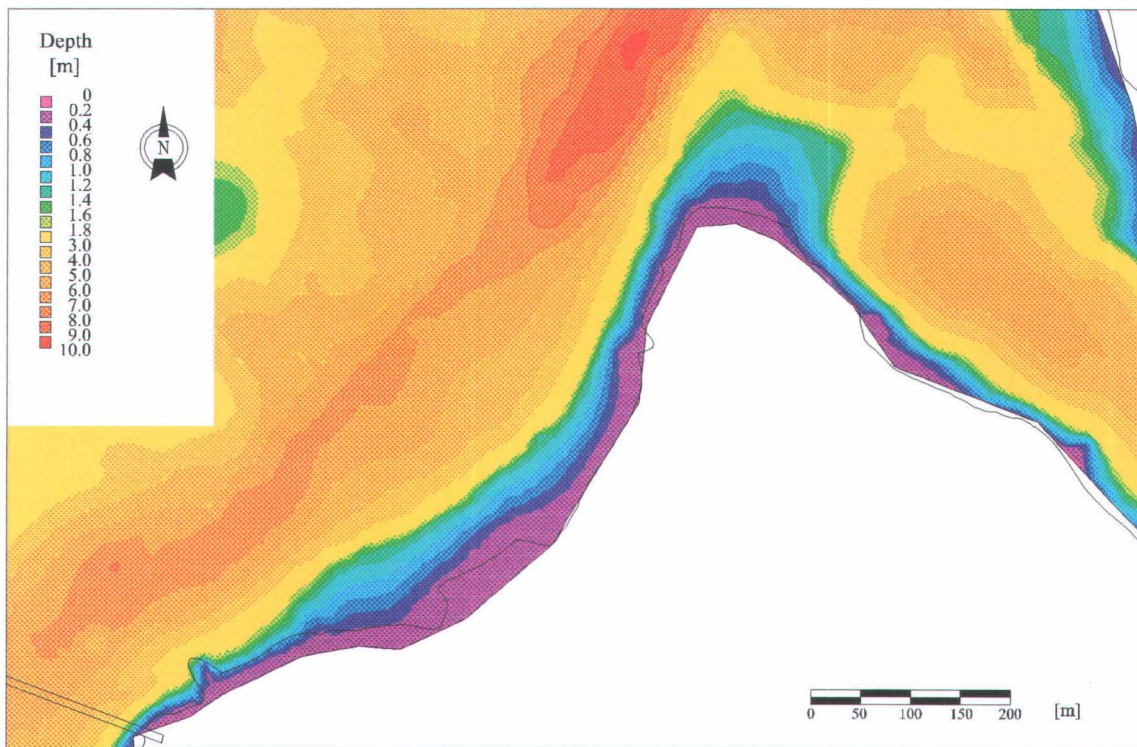


Figure 7 : Depth in the vicinity of Clark Island for the validation of the reference state.

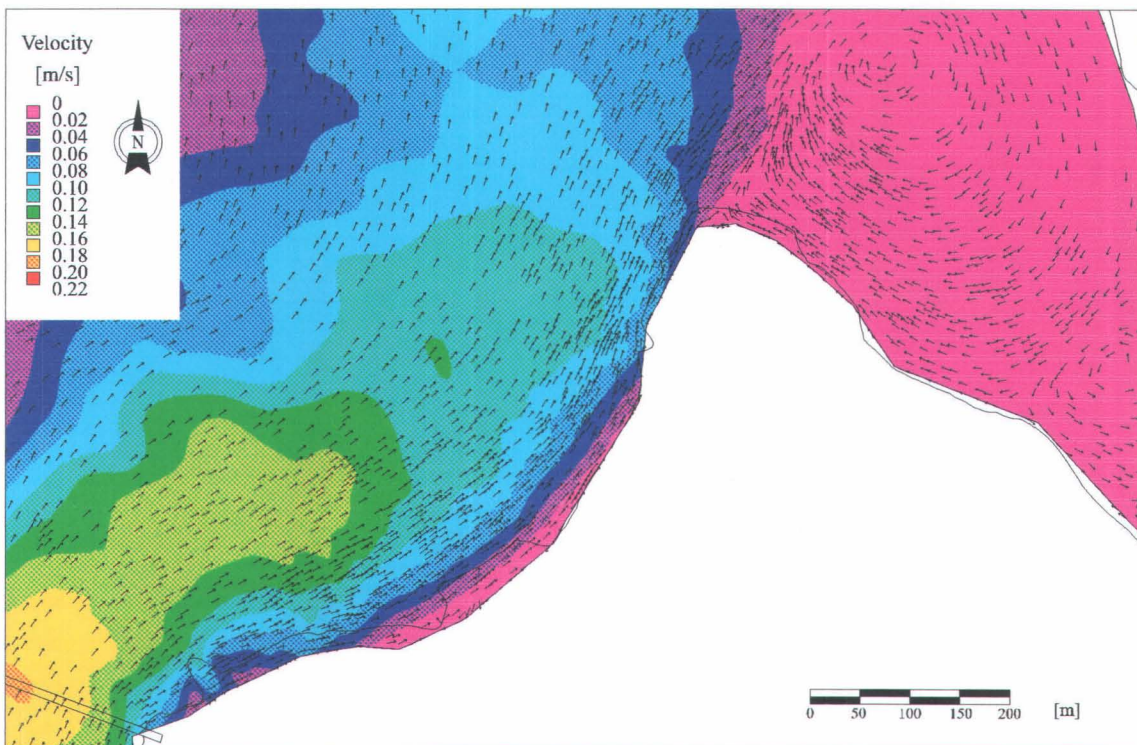


Figure 8 : Velocity in the vicinity of Clark Island for the validation of the reference state.

2.2.5. Integrating the capping structure

The topography around Clark Island was modified in the numerical field model (NFM) in order to take into account the capping structure (Figure 9, 10, 11 and 12). The elevation of the capping structure was set at 46.32 m - RIGL 55 (RIGL 85 : 46.40). A regular slope was given between the breakpoint on the capping structure and the topography at the lowest point of the capping structure.

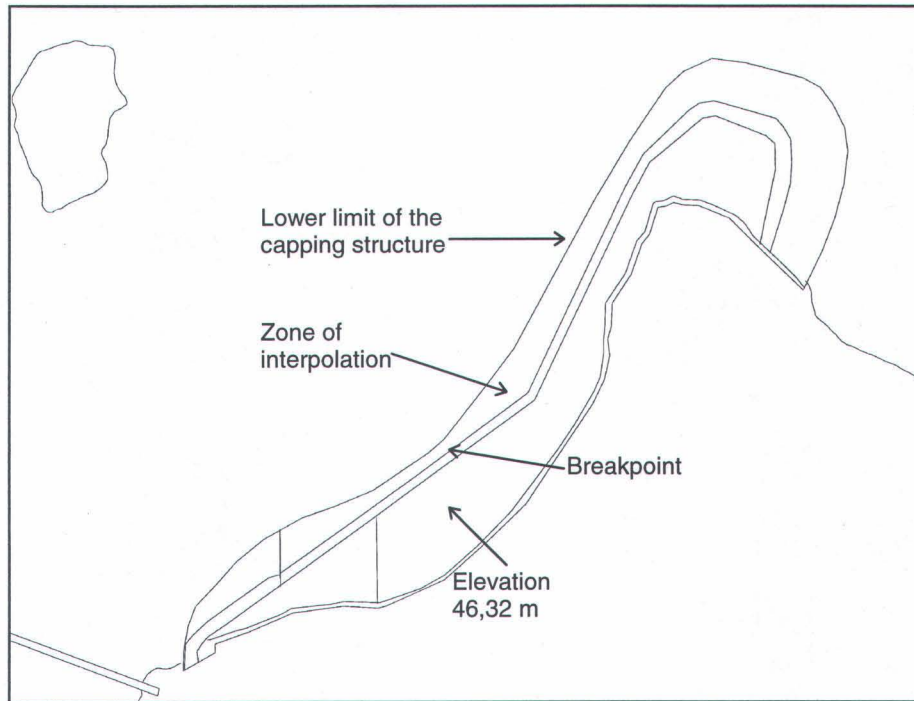


Figure 9 : Illustration of the capping structure.

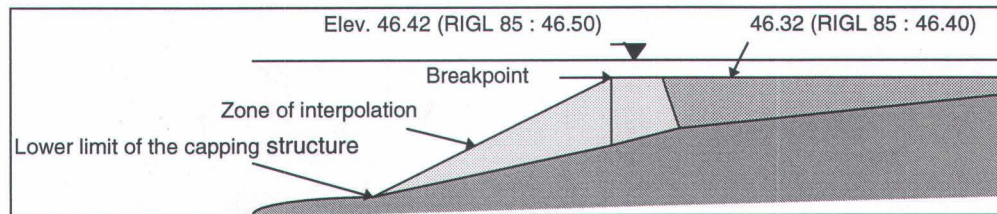


Figure 10 : Profile of the capping structure.

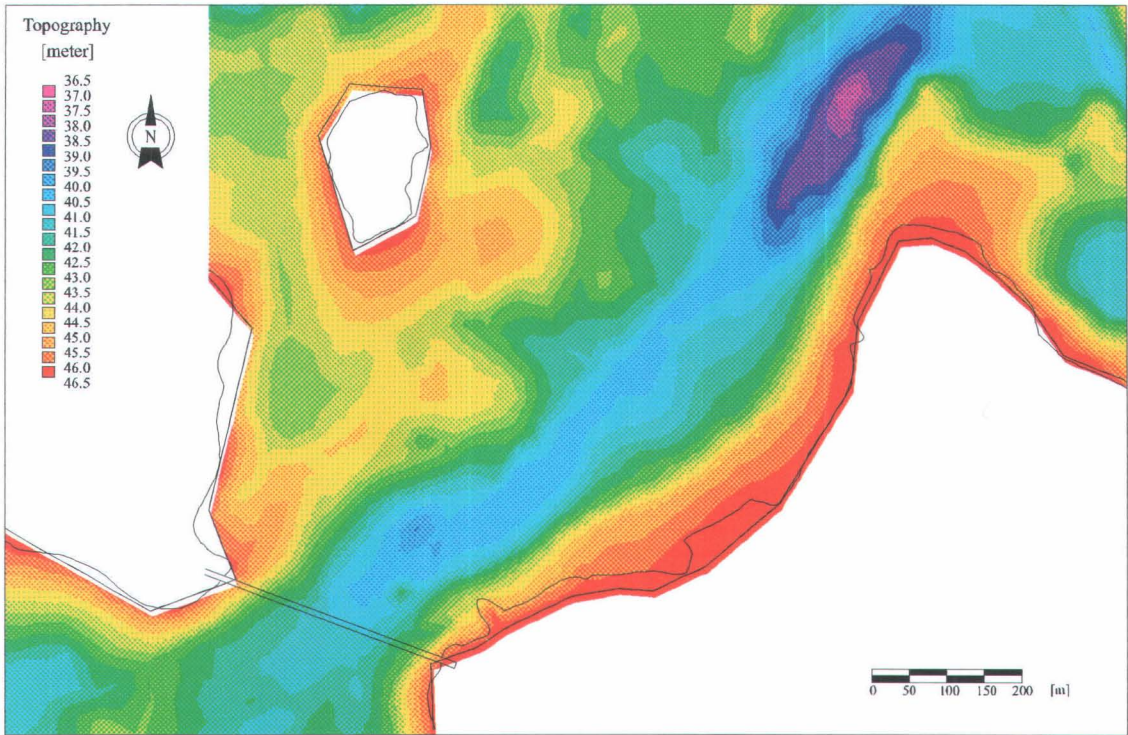


Figure 11 : Actual topography of the northwest shoreline of Clark Island.

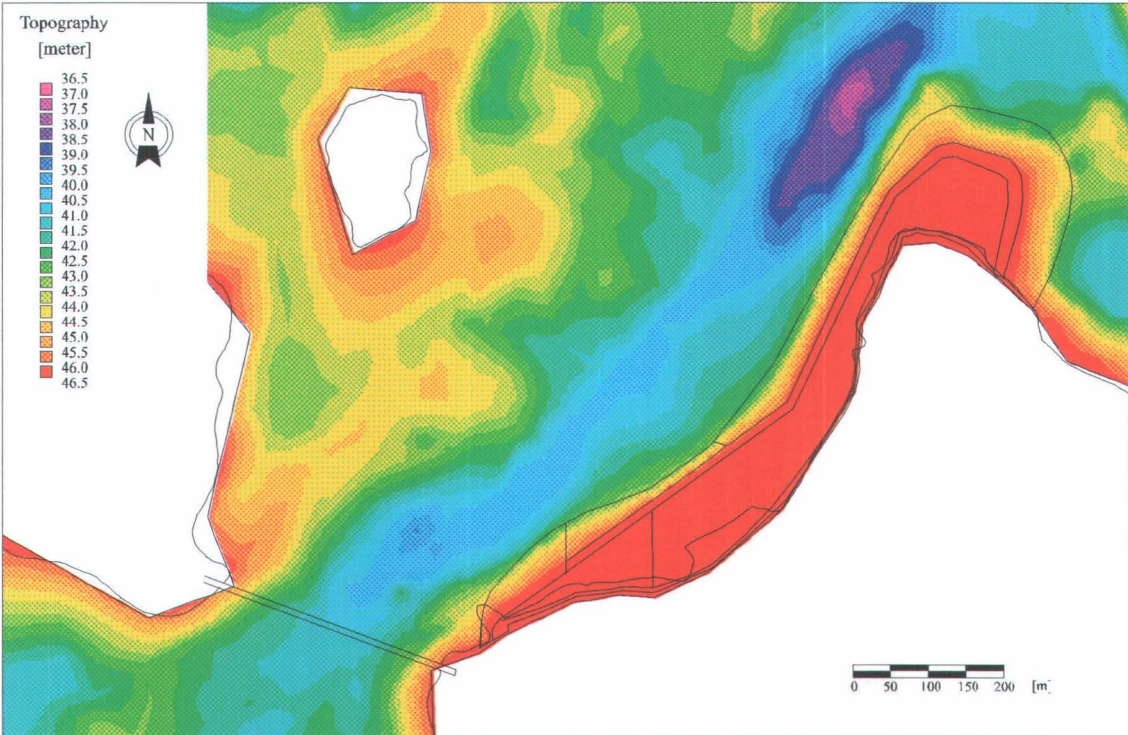


Figure 12 : Modified topography of the northwest shoreline of Clark Island taking into account the capping structure.

2.3. Results of hydrodynamic modeling

Hydrodynamic simulations were conducted for four distinct events.

- Reference state of October 1st with the capping structure : 8 200 m³/s (550 m³/s at the Coteau control structure) ;
- Average summer flow (Morin *et al.* 1994) with the capping structure : 7 800 m³/s (1000 m³/s at the Coteau control structure) ;
- Minimum summer flow with the capping structure : 6 500 m³/s (500 m³/s at the Coteau control structure) ;
- Maximum flow with the capping structure : 9 622 m³/s (4 533 m³/s at the Coteau control structure) ;
- Maximum flow without the capping structure : 9 622 m³/s (4 533 m³/s at the Coteau control structure).

2.3.1. Reference state : 8200 m³/s

The boundary conditions specified for the reference state (8 200 m³/s) were described in section 2.2.1. The same conditions were kept for the simulation at that flow value, integrating the capping structure : discharges of 350 m³/s and 200 m³/s through Coteau 1 and Coteau 3 respectively, along with a water level of 46.36 - RIGL 55 (RIGL 85 : 46.44) specified at the entrance of the Beauharnois canal. Figure 13 and 14 illustrate the depth and the velocity pattern for that flow in the vicinity of Clark Island. Vortexes are created above the capping structure and downstream from the capping structure, but the velocities remain fairly small.

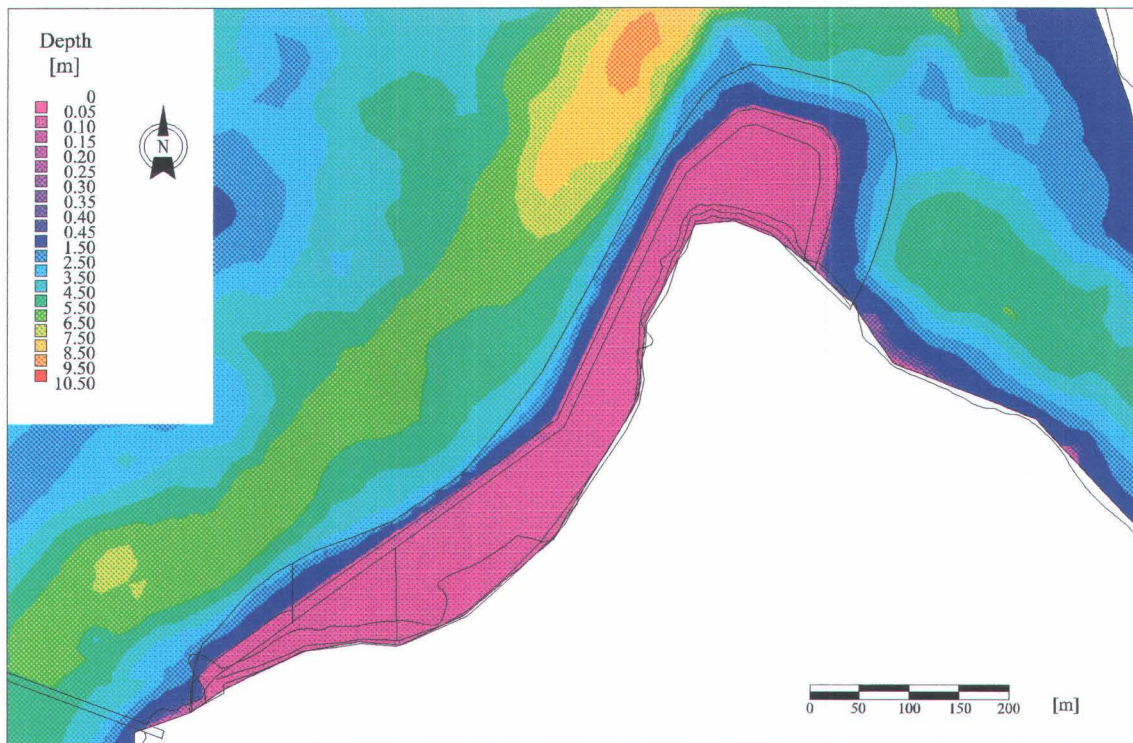


Figure 13 : Depth in the vicinity of Clark Island at a flow of 8 200 m³/s.

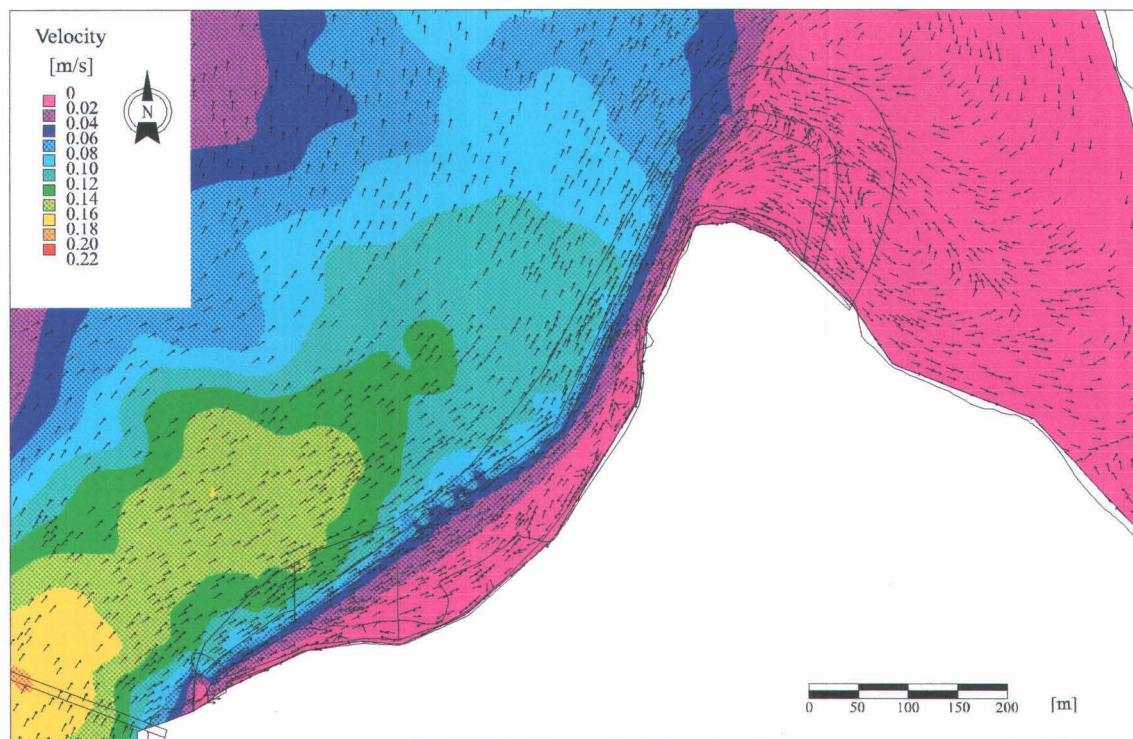


Figure 14 : Velocity in the vicinity of Clark Island at a flow of 8 200 m³/s.

2.3.2. Average summer flow : 7 800 m³/s

The boundary conditions for the average summer flow of 7 800 m³/s were set in order to satisfy Hydro-Québec's management policy as described in section 2.1.4. A discharge of 200 m³/s was specified at Coteau 3 with the remaining 800 m³/s flowing through Coteau 1. The water level was established at 46.36 - RIGL 55 (RIGL 85 : 46.44) at the Beauharnois canal in order to obtain a value close to 46.42 - RIGL 55 (RIGL 85 : 46.50) at Coteau-Landing. Figure 15 and 16 represent the depth and the velocity pattern at that flow value. A uniform depth of about 10 cm is found on the capping structure. A discharge of 1000 m³/s through the Coteau control structures produces velocities up to 0.3 m/s over the capping structure. Vortexes on and downstream of the capping structure are similar to those created at 8 200 m³/s.

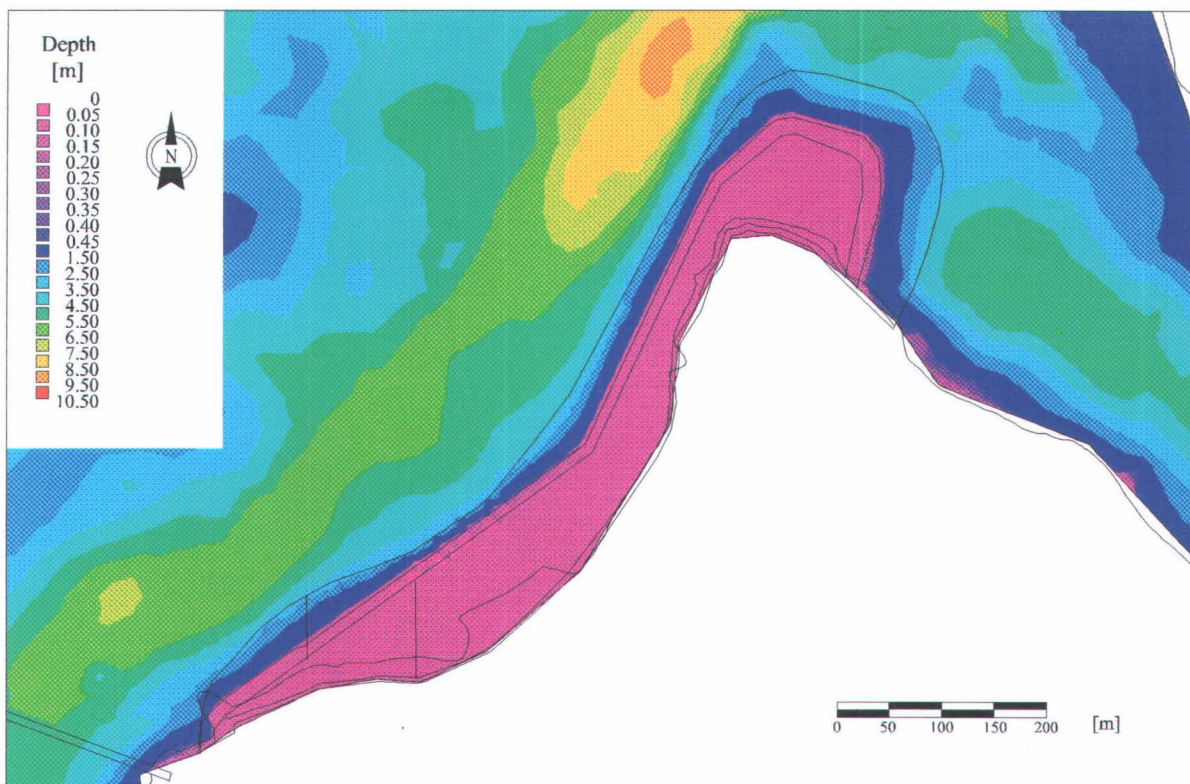


Figure 15 : Depth in the vicinity of Clark Island at a flow of 7 800 m³/s.

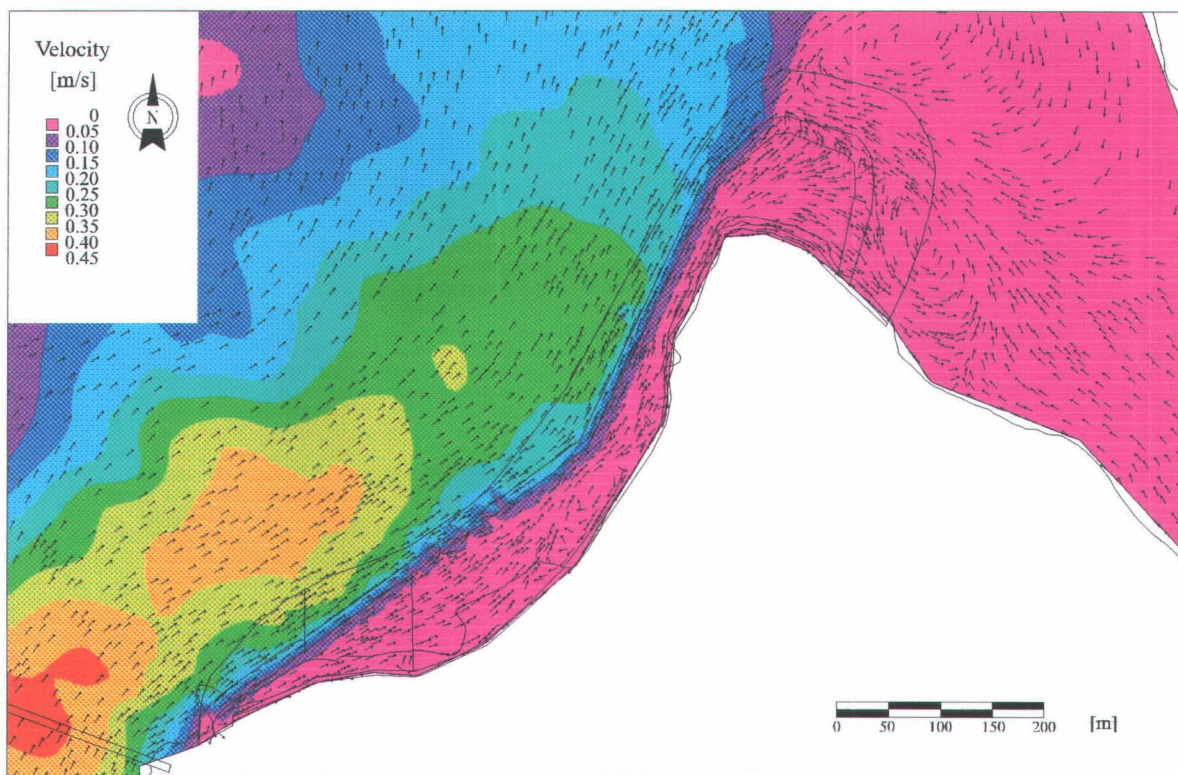


Figure 16 : Velocity in the vicinity of Clark Island at a flow of 7 800 m³/s.

2.3.3. Minimum summer flow : 6 500 m³/s

For the minimum summer flow event (6 500 m³/s) simulated in this study, the discharge at Coteau 1 was 300 m³/s and the discharge at Coteau 3 was 200 m³/s. The water level specified at the entrance of the Beauharnois canal was the same as for the first three simulations, i.e. 46.36 m. The depth and the velocity pattern are shown in figures 17 and 18. Both the depth and the flow pattern are similar to the results obtained for the reference state since the discharges at the Coteau control structure are the same.

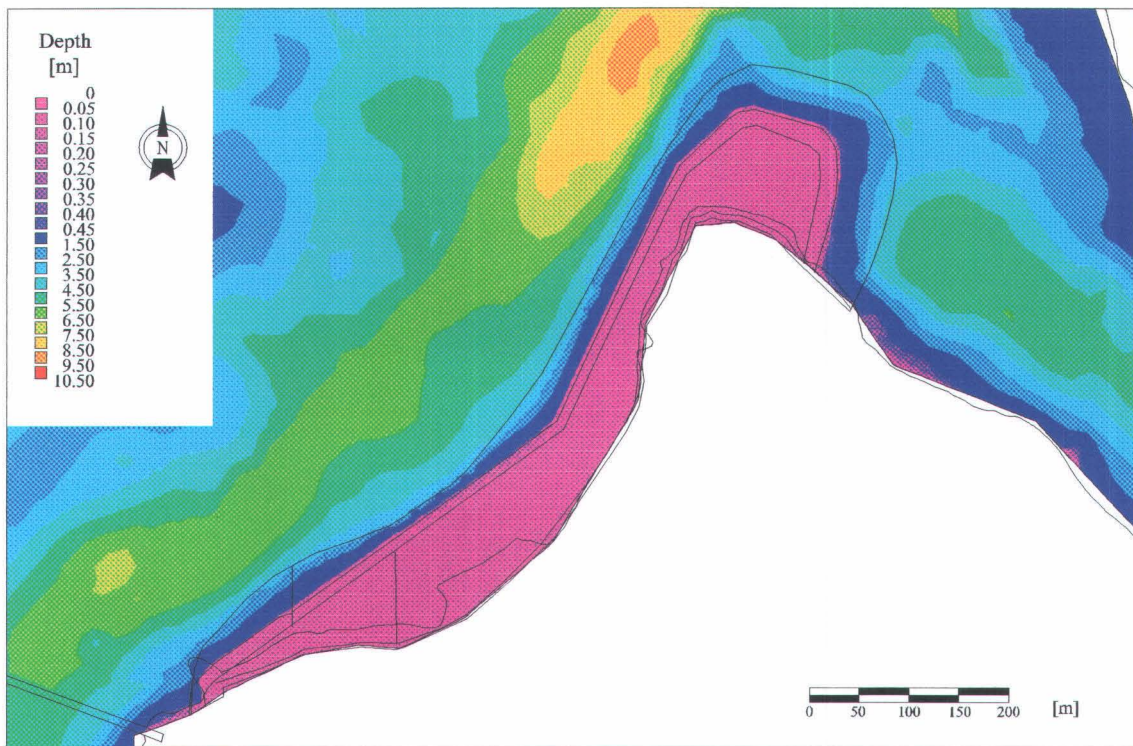


Figure 17 : Depth in the vicinity of Clark Island at a flow of 6 500 m³/s.

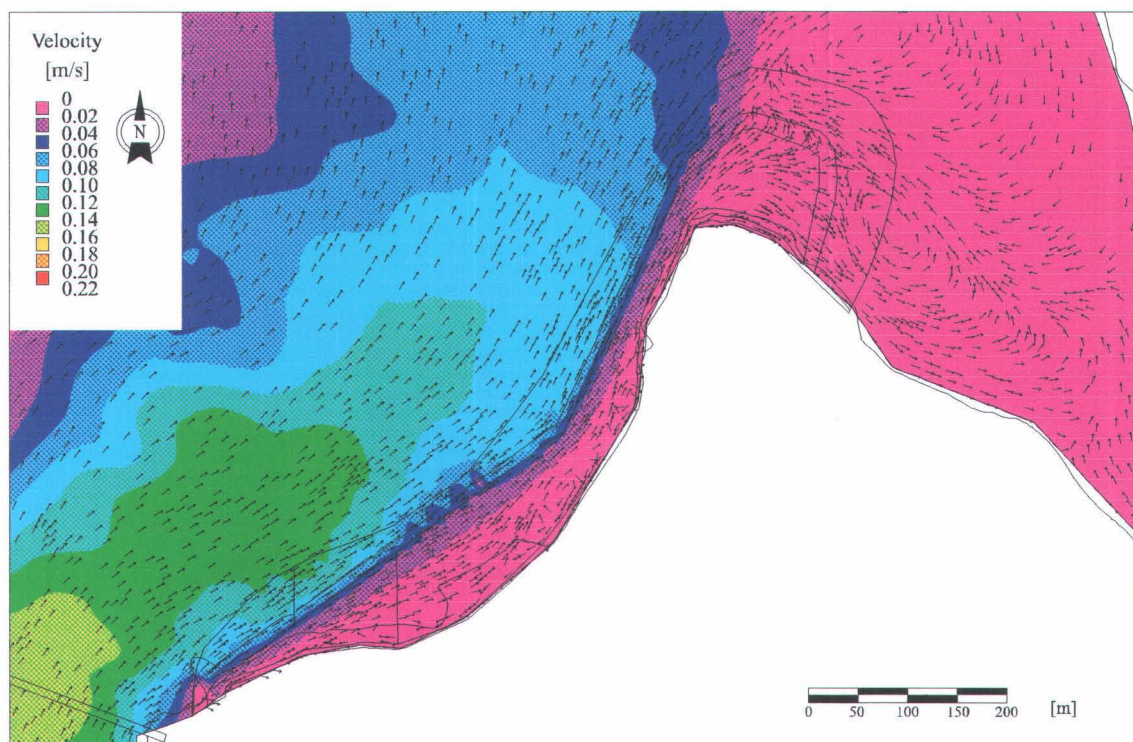


Figure 18 : Velocity in the vicinity of Clark Island at a flow of 6 500 m³/s.

2.3.4. Maximum flow : 9 622 m³/s, with the capping structure

According to Hydro-Québec's management policy, there is a discharge of 2 687 m³/s passing through Coteau 1 when the flow at the Coteau control structures is 4 533 m³/s. Thus the discharge at Coteau 3 is 1 846 m³/s. The water level at the Beauharnois canal is estimated at 46.37 m (RIGL 55) at that specific flow value. As illustrated in figures 19 and 20, the water level at this particular flow is fairly low in the vicinity of Clark Island, leaving the capping structure uncovered. This can be explained by the fact that the water surface slope has to be rather steep to allow 4 500 m³/s through the Coteau control structures.

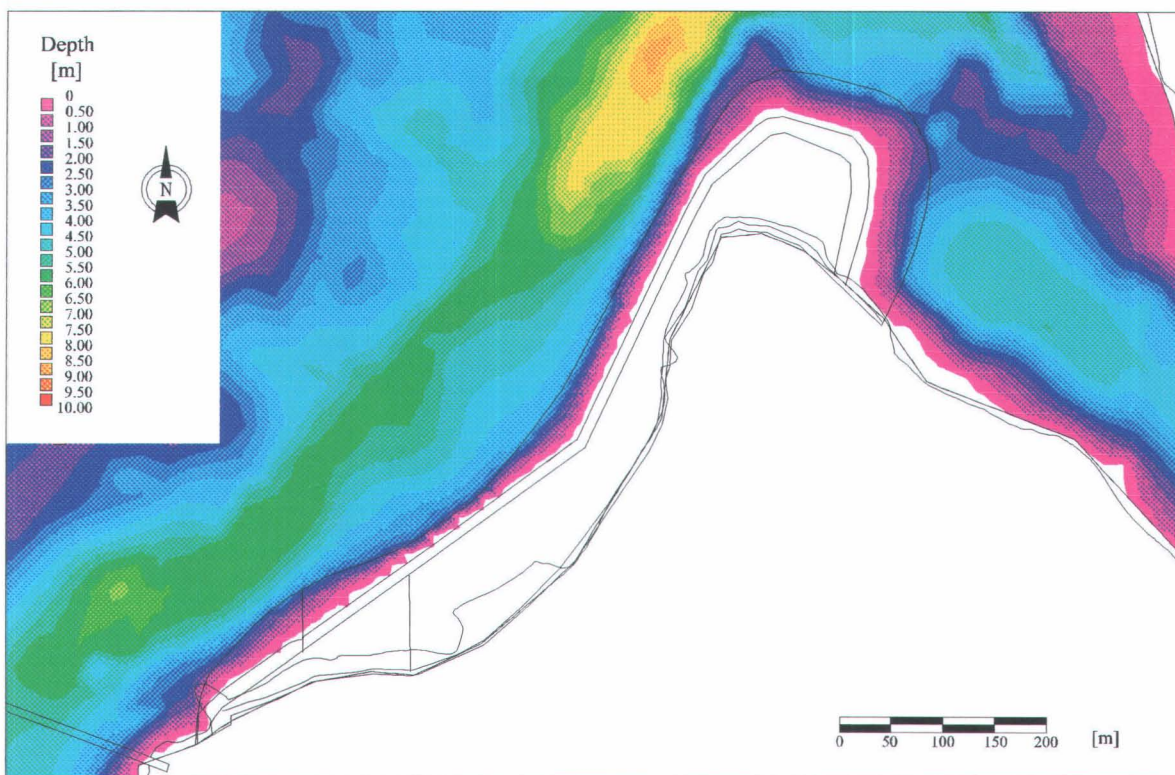


Figure 19 : Depth in the vicinity of Clark Island at a flow of 9 622 m³/s with the capping structure.

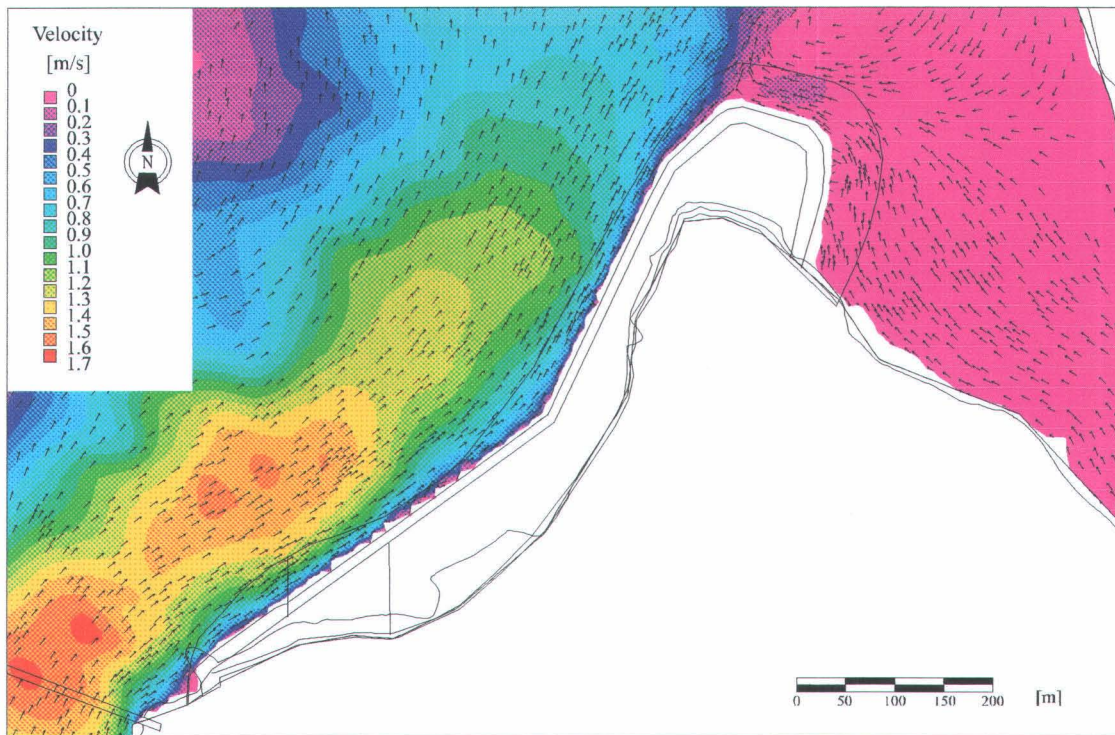


Figure 20 : Velocity in the vicinity of Clark Island at a flow of 9 622 m³/s with the capping structure.

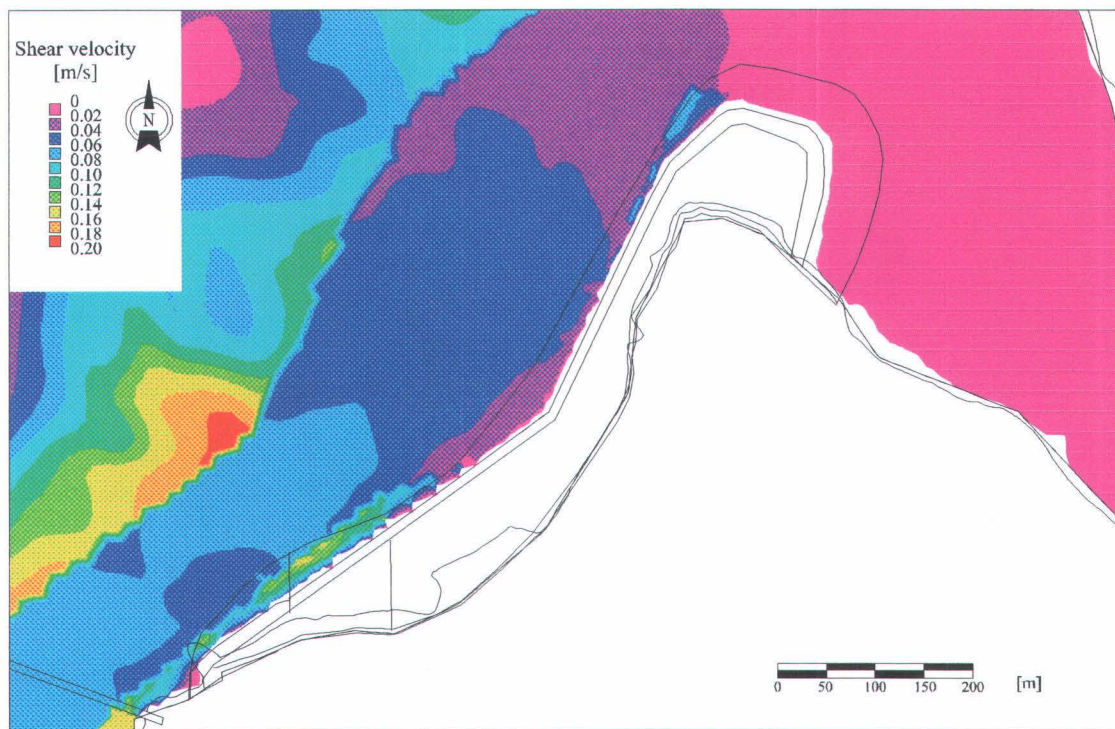


Figure 21 : Shear velocity in the vicinity of Clark Island at a flow of 9 622 m³/s with the capping structure.

2.3.5. Maximum flow : 9 622 m³/s, without the capping structure

An additional simulation has been made for a flow of 9 622 m³/s in order to analyze the current pattern and the shear velocities on the shore of the island in the absence of a capping structure. Figure 22 illustrates the depth whereas figure 23 illustrates the currents around Clark Island. This simulation represents flow conditions that are actually relatively rare ; however before the erection of the Coteau dams, the flow conditions around Clark Island were similar to these simulations. The shear velocities, which are illustrated on figure 24, reach a value of more than 0.16 m/s on the shore of Clark Island.

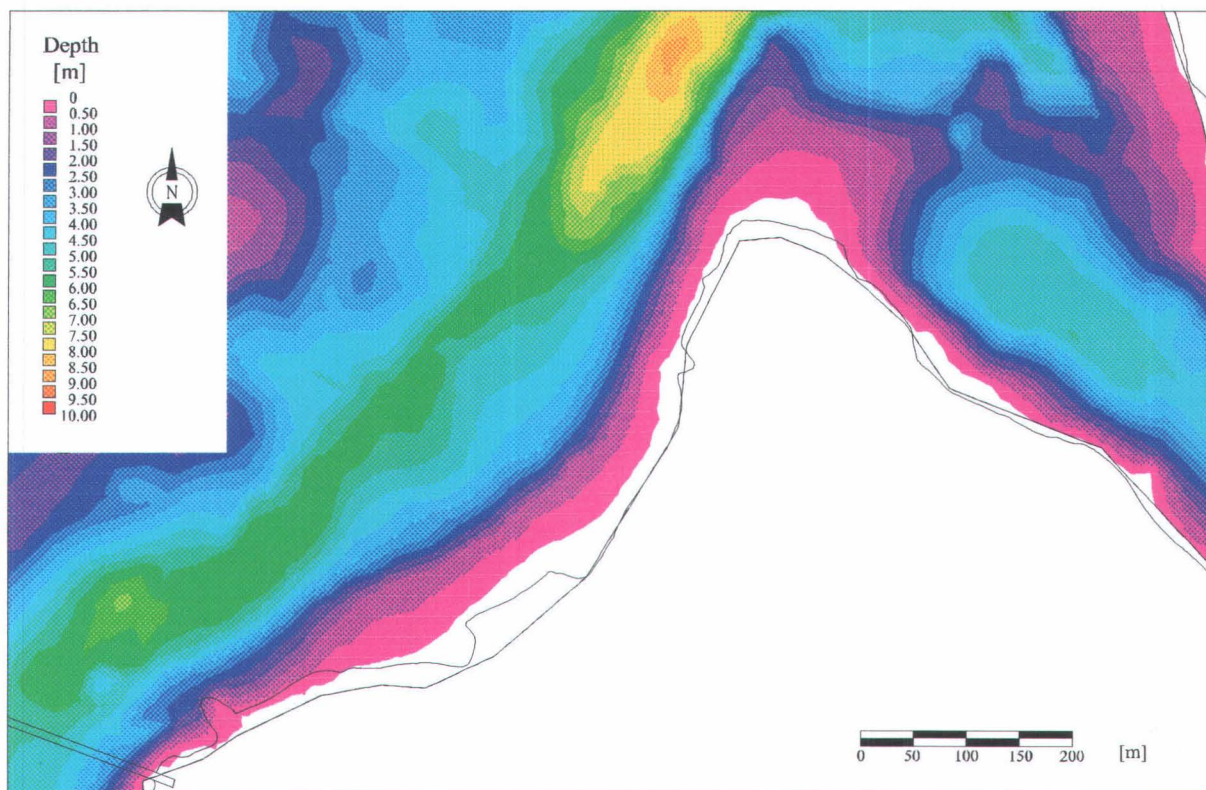


Figure 22 : Depth in the vicinity of Clark Island at a flow of 9 622 m³/s without the capping structure.

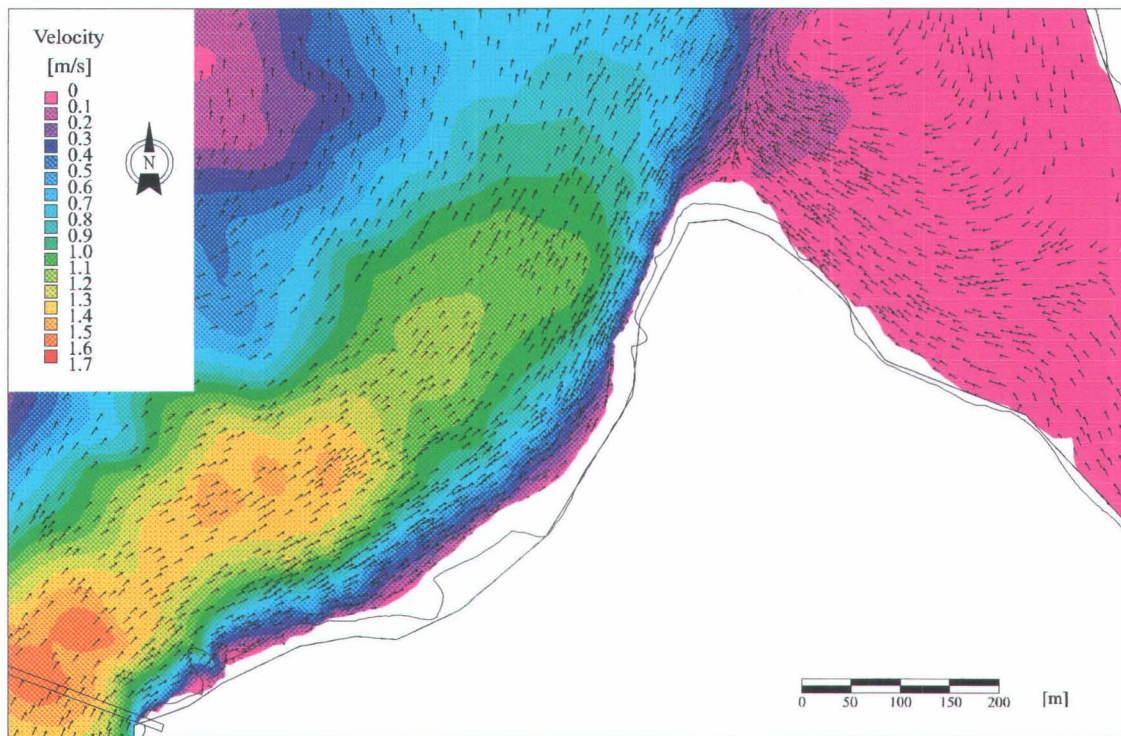


Figure 23 : Velocity in the vicinity of Clark Island at a flow of 9 622 m³/s without the capping structure.

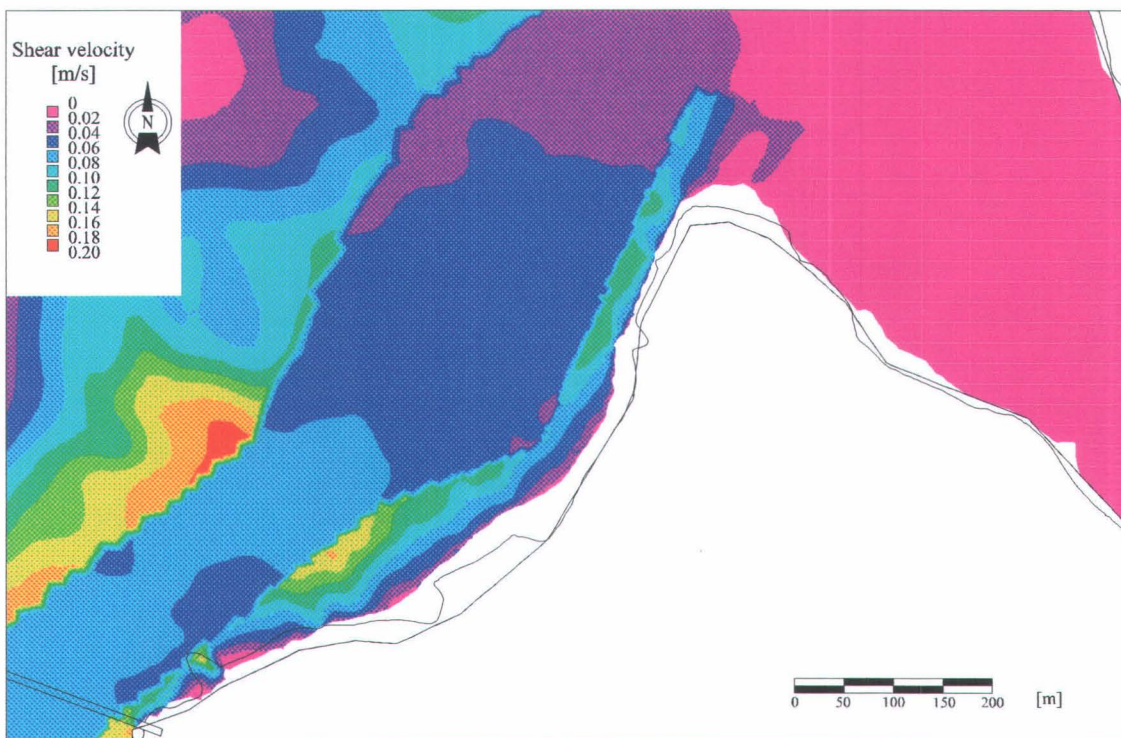


Figure 24 : Shear velocity in the vicinity of Clark Island at a flow of 9 622 m³/s without the capping structure.

2.3.6. Impact of the capping structure

The maximum shear stress induced by currents to which the capping structure will be exposed is relatively well represented by the event simulated with a flow of $4\,533\text{ m}^3/\text{s}$ at Coteau structures. Figure 21 presents the distribution of calculated shear velocities in the study area. The maximum value affecting the structure is 0.18 m/s . This value is relatively small and causes no damage to the structure.

The implementation of a capping structure on the northwest shoreline of Clark Island will have a local influence on water depth and velocities. Figure 25 shows the difference between the velocities simulated with and without the capping structure when the total discharge is $8200\text{ m}^3/\text{s}$. The velocities occurring on the southwestern extremity of the capping structure are increased by 0.05 m/s , whereas the velocities over the capping structure are almost null. It is important to note that there is no reduction of current velocities within the bay on the eastern side of Clark Island.

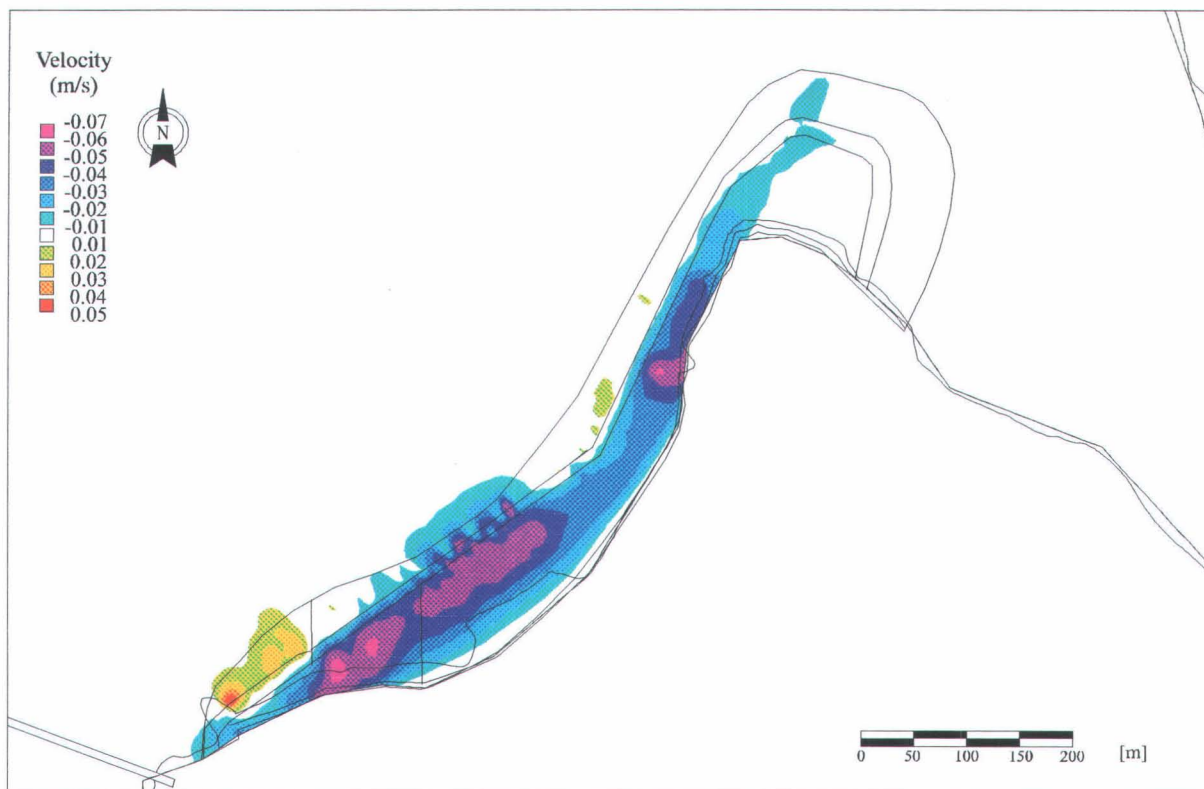


Figure 25 : Differences between velocities simulated with and without the capping structure at a flow of $8200\text{ m}^3/\text{s}$.

Discharges passing through the Coteau control structures have an important effect on water level in the vicinity of Clark Island. Table 5 shows water levels simulated by the hydrodynamic model at different points of interest.

Table 5 : Water level calculated by the hydrodynamic model at different points of interest

Discharge ⁽¹⁾ (m ³ /s)	Water level calculated (m) (RIGL 55)			
	Upstream boundary	Beauharnois canal	Coteau-Landing	Capping structure
8 200 (550)	46.60	46.36	46.43	46.40
7 800 (1 000)	46.58	46.36	46.42	46.37
6 500 (500)	46.51	46.36	46.40	46.39
9 600 (4 533)	46.51	46.37	46.40	45.96

(1) The value in parentheses corresponds to the flow passing through the Coteau control structures

The water level at the upstream boundary was determined by the simulations. The first noticeable fact observed from the values calculated by the model is that the water level at the upstream boundary is the same for both the maximum and minimum flow. The low water level for the maximum flow can be explained by the fact that the gates at the Coteau control structures were open, releasing more water. As a consequence, the portion of the flow diverted to the Beauharnois canal was low compared with all other events simulated inducing a more gentle water surface slope.

The water level at the Beauharnois canal was specified as the downstream boundary condition whereas the water level at Coteau-Landing was estimated by the model. The latter value is also influenced by the discharge diverted to the Beauharnois canal. A low discharge in the Beauharnois canal for a same total discharge upstream corresponds to a lower level at Coteau-Landing.

According to the simulations for the 9 622 m³/s discharge, a high discharge at the Coteau control structures has an important local impact on the water level. In fact, the water surface slope created to allow a flow of 4 500 m³/s through the Coteau control structures reaches a value of 0.05% in the vicinity of Clark Island.

3. Wave modeling

3.1. Data

3.1.1. Topography

Accurate topographic data sets are essential to obtain adequate wave simulations in shallow water. The same data set used for hydrodynamic modeling was also used for wave modeling. Two field elevation models were used ; the first represents the present conditions (without the capping structure) and the second represents the conditions after implementation of the planned capping structure.

3.1.2. Wind statistics and choice of event

Wind statistics performed in Morin *et al.* (1994) and in an INRS-Eau report on a Lake St. Francis beach stability (Boudreau et al 1995) were used to choose the appropriate wind direction and speed. As reported in Morin *et al.* (1994), dominant winds in the area are blowing in an East-West direction. They are stronger during the fall and the spring, and there are no extreme winds (45-55 km/h) during the summer. Generally, the stronger winds are westerlies, on an approximately equal frequency from the northwest, the west and the southwest. However during the spring, strong winds can also blow from the east. Statistics from five years of hourly data show that extreme wind speed reached a maximum of 55 km/h in the area. Extreme winds (45-55 km/h) occur only 5 days per year on average and we believe that 60 km/h winds represent a rare but « structuring » event, because it can have a significant impact on sedimentation and on resisting material (plants and structure).

For modeling purposes, we elected to simulate a maximum effect of strong winds during the fall. This corresponds to winds blowing from the northwest, the west and the southwest at a speed of 60 km/h. For the Clark Island site, these wind directions have the longest fetches. We also used the calibration event (October 1st, 2nd 1996) with a total discharge of 8200 m³/s (350 m³/s at Coteau 1 and 200 m³/s at Coteau 3) for current and water level conditions as an input to the wind model. This event was also simulated with and without the capping structure, allowing to use the same event for wave simulations (with and without the capping structure). Three directions and two bathymetric conditions were simulated for a total production of six wave fields.

3.2. Modeling the waves

3.2.1. Wave model HISWA

Wave models capable of simulating accurately shallow water waves are not common. In the physical context of Clark Island, strong currents, complex bathymetry and abundant vegetation are affecting wave behavior. Wind growth, wave propagation (refraction) and wave dissipation from bottom friction, from white-capping, from aquatic vegetation and from currents are the main

parameters of HISWA (HIncast Shallow water Wave), a model developed by Delft University of Technology, Netherlands (see Booij et al. 1993).

3.2.2. Discretization

HISWA uses finite differences for calculation. Regular rectangular grids are structuring the calculation parameters such as bathymetry, currents, and water levels. Different grids with a different mesh size can be used for data input, calculation and output. Local refinement is done through a « nesting » method that allows to resimulate on a finer grid with known boundary conditions. When done manually, these grids become rapidly fastidious to produce and manage. The MODELEUR was more than useful for grid production, interpolation and visualization.

Two different grids were produced for either the situations without and with the capping structure. The first grid that covers a portion the eastern part of the lake is composed of 58 000 nodes with a mesh size of 25 m. A local refinement of the grid, a nesting grid, was built with 64 000 nodes and a mesh size of 5 m. This nested grid covers the capping structure and the surrounding area.

3.2.3. Initial and boundary conditions

For all HISWA simulations, boundary conditions were defined mainly by the presence of land. The model was set to take into account white-capping and bottom friction. The width of the directional sector was fixed at 120 degrees, i.e. 60 degrees on each side of the main direction of propagation. The spectral domain was divided in 90 intervals for a spectral directional resolution of 1.33 degrees/interval (120/90). Most of the boundaries of the calculation grids were limited by land ; only the southwestern side was an open boundary. Simulations of southwesterly winds consider a shorter fetch than actually occurs. Considering that the bridges most certainly break the propagation of waves and that the study site is clearly protected by the narrow channel between the islands, we believe that the southwest wind simulation is close to reality.

3.3. Results of wave modeling

The modeling results can be visualized for the three simulated conditions both with and without the capping structure. Wave simulations can produce several output variables ; we have selected the shear velocity created by the orbital movement of waves because it represents the direct effect of waves on structures, on substrate and on plants. In order to simplify the analysis, we have produced two images containing the maximal shear velocity of each node for the three simulations. One node has three attributes of shear velocity produced by the three simulations ; a simple calculation with the MODELEUR allowed us to retain the maximum value for each node of the grid. Thus we obtain two images of the maximal shear velocity which can be observed in the area, one without the capping structure and the other with the structure in place.

3.3.1. Without the capping structure

The modeling results presented in figure 23 show the spatial distribution of the shear velocities produced by waves at the study site. Shear velocity induced by waves is very low in the deep water of the main channel and in the relatively protected area of the bay on the eastern side of Clark Island. Relatively strong shear stress occurs on the northwestern side of the island, at the break in slope and directly on the shore. Maximum shear velocity is 0.8 m/s.

3.3.2. Ground-truthing observations

There are no wave measurements available for the area. Thus the quantitative validation of the model is not possible, but some qualitative clues can be gathered in the field. Several field observations along the local shoreline confirm the occurrence of important wave erosion on the northwestern side. On June 17th 1997, we observed significant erosion along the northwestern shore ; the root systems of shore trees were severely exposed, tree stumps still in living position were present several meters from the shore, and small but active erosion banks occurred in the northern part of the island. Local substrate distribution also reflects important wave action ; clean sand occurs in the faint bay on the northwest side, coarse material (cobbles and boulders) is present in the northern area.

3.3.3. With the capping structure

The modeling results presented in figure 24 show the spatial distribution of the shear velocity over the planned structure. Differences with the simulation without the capping are very localized, occurring only over the modified zone. Shear velocities in deep water offshore of the island are exactly the same. Shear velocities are significantly smaller on the east side of the island, the capping structure acting as a protective barrier. On the capping structure, the entire energy that was dissipated over all of the area is now concentrated on the break in the slope of the structure. This concentration of wave energy induces shear velocity reaching 1.10 m. The energy is almost entirely dissipated after only a few meters over the capping structure ; only a small portion is present inside the capping.

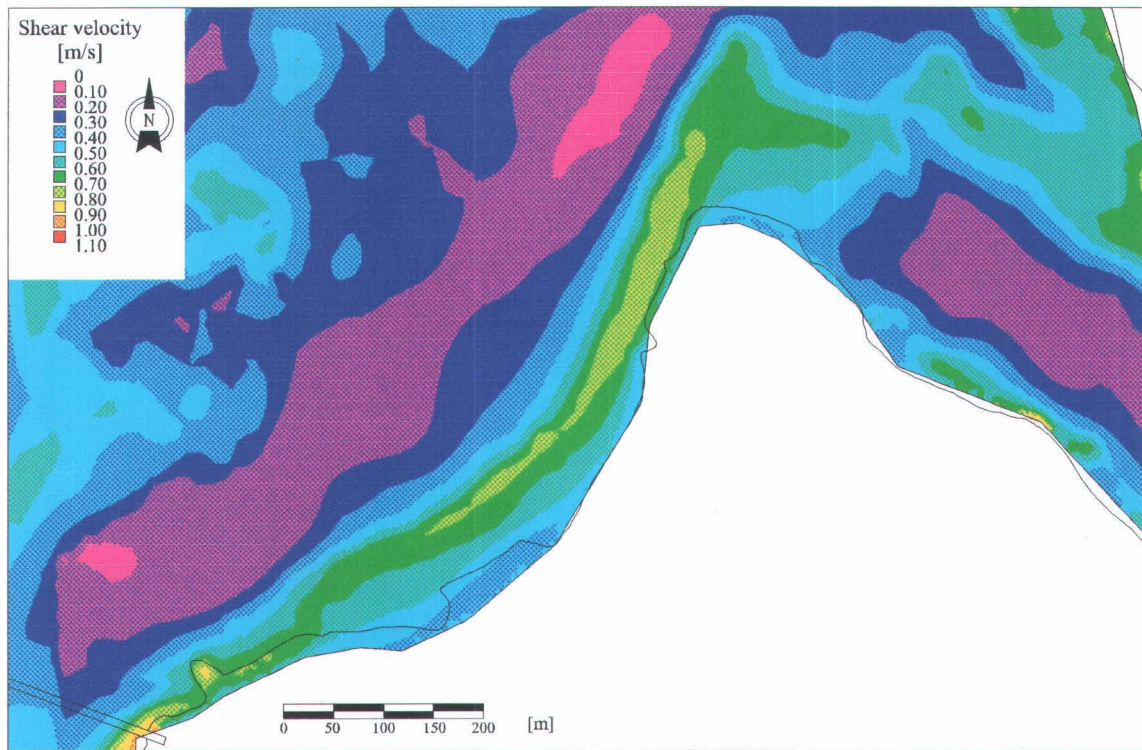


Figure 26 : Wave induced shear velocities without the capping structure.

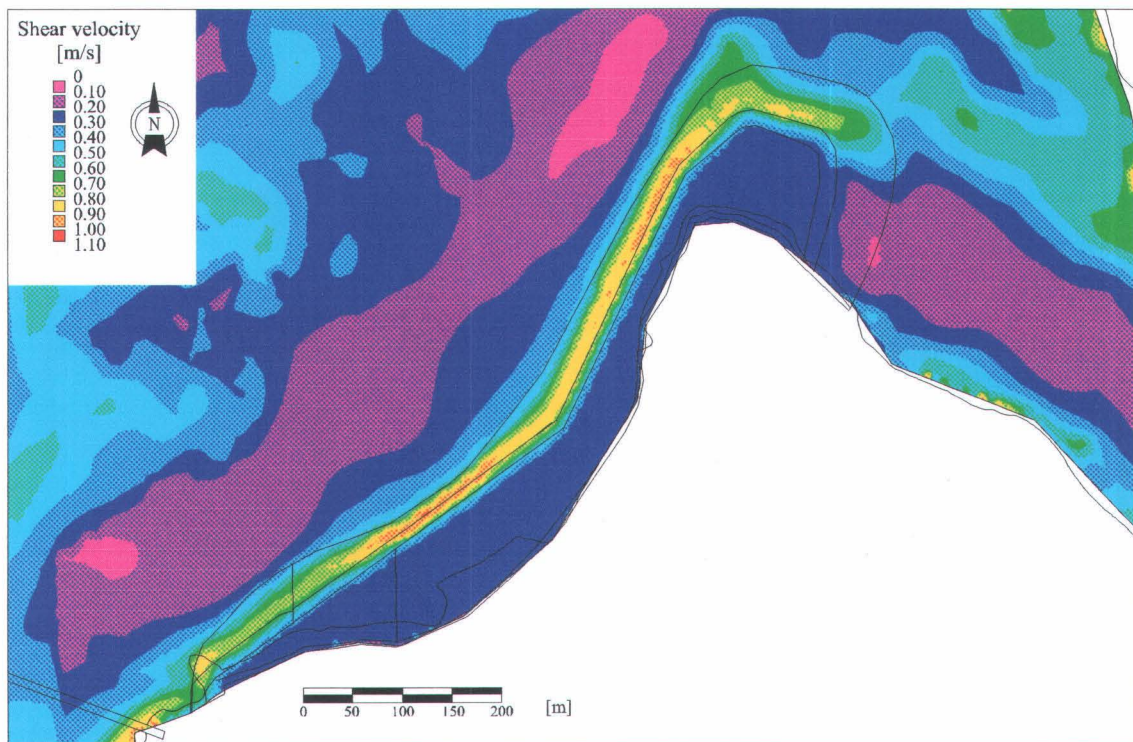


Figure 27 : Wave induced shear velocities with the capping structure.

4. Plants habitat

Habitats of emergent aquatic plants are controlled mainly by three abiotic factors : waves, substrate and water depth. Velocities can also play a minor role along with the concentration of nutrients. Waves control the occurrence of plants by exerting a mechanical stress on stems and leaves (Weisner 1991). Water depth is a limiting factor because of the hydrostatic pressure inhibiting the gaseous transportation to the roots and because of the energy necessary for shoots to reach the water surface (Yamasaki 1984 ; Spence 1982). Substrate plays two different roles : it serves as a nutrient pool for plants and it helps stabilize and anchor the rooting system. Nutrient rich substrates are capable of supporting a larger biomass. Root penetration is essential ; emergent plants are often found on « recently » deposited fine material.

4.1. Methodology of plants analysis

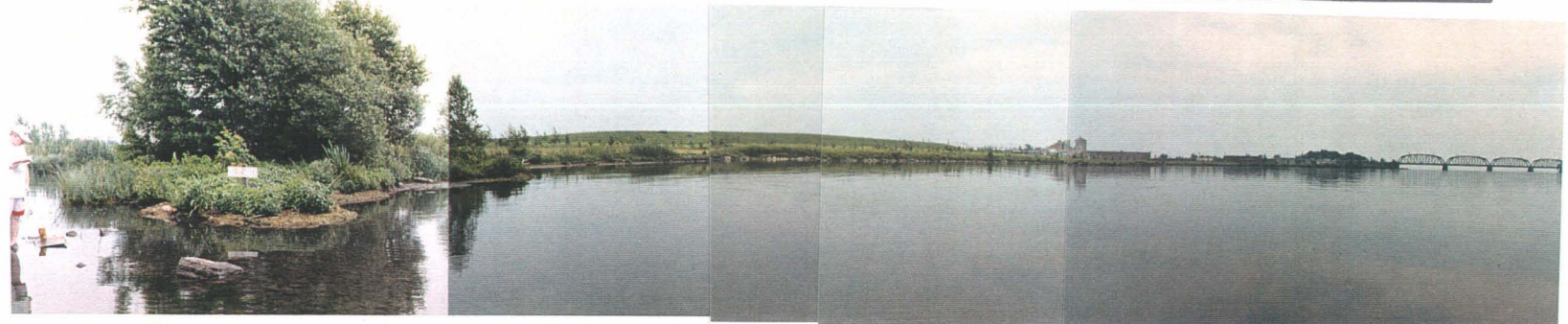
The methodology used for the assessment of emergent aquatic plants is relatively simple and follows a methodology defined for submerged aquatic plants by Morin *et al.* (1996). As mentioned above, abiotic conditions are determinant for species distribution. Very little is known about abiotic preferences of emergent species. Literature data are scarce and allow only for very broad generalization. In order to understand and describe properly these abiotic preferences, we conducted a systematic vegetation field survey (identification and distribution). Plant distribution was mapped, and sediment thickness was measured and its composition was identified.

Combining the distribution of various plant species with the results of wave simulations and of the hydrodynamic model, we were able to calibrate the relative resistance of every species to wave action and to water depth. It was then possible to predict relatively well the future distribution of plant habitats on the new structure, knowing which plant species would thrive better under various wave energies, water depths and substrate compositions.

4.2. Field observations and habitat

Two field trips were done : a first visit on June 17th to sample plants on the northern part of the island, and a second visit on July 13th when plants were more developed, flowers were present and taxonomic identification was easier.

Several species are present in the northeastern part of the island. Figure 28a, taken on July 13th, shows a wide angle view of the site with most of the species present in the area. From the left side close to the horizon line, *Scirpus lacustris* forms a low density community. Immediately to the right of the *Scirpus* zone (figure 28a), a dense formation of *Typha angustifolia* occurs ; closer to shore, *Equisetum fluviatile* and *Scirpus lacustris* are present, while on the shore *Carex aquatilis* and *Scirpus fluviatilis* are abundant. On the left side of figure 28, *Nymphaea* sp. is common. Figure 28b shows the northern-most point of the island viewed from the lake.



a)

b)

c)

Figure 28 : Field photos of island shore.

Erosion induced by wave action has exposed tree roots, and tree trunks are now observed in the lake. Figure 28c shows the actual onshore vegetation of the northwestern part of the island. Note the very coarse substrate around the point and the absence of emergent plants on this part of the island due to strong wave action.

4.2.1. Description of abiotic factors

We retained five species of emergent plants for which we described their habitat preferences. Table 6 presents the habitat preferences for these species. Although *Typha latifolia* was not observed in the area, we believe that it will certainly be one of the dominant species of the final design because of its preference for shallow and protected areas.

Table 6 : Habitat preferences of selected species

	Wave exposure ^A (relative index)	Water depth ^B	Substrate	Simulated wave (shear stress from 60 km/h wind m/s)	Simulated Velocities (m/s)
<i>Carex aquatilis</i>	3 Grows in protected area	-10 cm à 0 cm (average of -5 cm) ³	rich in organic matter ² 10 cm to 40 cm	0.4 to 0.5	less than 0.2
<i>Scirpus lacustris</i>	10 Good resistance to wave action	10 cm to 140 cm	Muddy or sandy 10 cm to more than 50 cm	0.5 to 0.7	less than 0.2
<i>Scirpus fluviatilis</i>	1 Grows in relatively protected area with no current ¹	0 to 30 cm	Muddy 10 cm and more	0.3 to 0.4	less than 0.2
<i>Typha angustifolia</i>	8 Good resistance to wave action	40 cm to 100 cm	Fine and rich in organic matter ² 30 cm and more	0.3 to 0.5	less than 0.2
<i>Typha latifolia</i>	0 Grows in very protected area	-10 cm to 40 cm	Fine and rich in organic matter ² 40 cm and more	unknown probably 0	unknown probably 0

^A Arbitrary scale based on field observations from 0 (no wave) to 10 (maximum wave)

^B Positive values indicate values over the interface roots/stems (soil level)

¹ From Fleurbec, 1987

² From Couillard et Grondin, 1986

³ From Auclair et al., 1973

In table 6, wave exposure corresponds to field interpretation of the local wave energy. We use an arbitrary scale ranging from 10 for plants occurring in the most energetic environments to 0 for plants growing in protected zones. Water depth corresponds to the distance from the water level (measured positively downward) to the bottom/water interface or soil/air interface. Suitable substrates are mainly rich in fine material and in organic matter. Simulated wave shear stress where plants occur is also used to segregate and quantify field observations. As expected, velocities are relatively low where plants grow. Generally, *Scirpus lacustris* resists better to wave action and should be used for revegetalization in the area exposed to dominant winds. At the

other end of the spectrum, *Typha latifolia* grows in shallow water and is neither resistant to current nor to waves and should be used only in protected areas.

4.3. Choice of plants for revegetalization

Several solutions can be proposed for revegetalization of the capping structure. Choosing the best solution depends on the knowledge and the values that are put forward. One of the most recognized values for ecosystem management is the biodiversity concept (see Dodge and Kavetsky 1995). Globally, the larger the number of species sustained by a given ecosystem, the greater the biodiversity. In order to maintain species diversity, habitats have to be diverse in terms of water depth, wave energy and water circulation. Colonizing plants must be a good source of food.

Three species were retained for the revegetalization of the site : *Scirpus lacustris*, *Typha latifolia*, and *Typha angustifolia*, for the following reasons. These plants cover a wide spectrum of habitat characteristics typical of the study site ; they are common on disturbed grounds (especially *Typha* sp.) ; they are part of the natural ecosystem of the area. These species were also chosen for several qualities other than their habitat tolerance. *Scirpus lacustris* is an important source of forage for waterfowl and it provides interesting nesting sites for several birds species (Fleurbec 1987). *Scirpus lacustris* stems and rhizomes are eaten by geese and muskrat ; their seeds are particularly appreciated by waterfowl. *Typha latifolia* is also an important source of food for waterfowl and mammals.

4.4. Habitat characteristics the capping structure

The most important abiotic variables for emergent plants and therefore for most of other biota were simulated and analyzed for the planned capping structure. As described earlier, emergent plants in this type of environment are mainly influenced by waves, current, water depth and substrate characteristics. Considering that this structure is to be built, the type of substrate available for plants is not relevant because it is possible to plan its nutrient level and its physical properties. As modeled, current velocities are not discriminating for plant species in the sense that the range of speeds within the structure is suitable for all three selected plant species. Waves and water depth appear then to be the controlling factors for plant distribution within the planned structure.

Waves shear stress within the structure is almost the same everywhere ; only the break in slope at the margin of the structure has a different wave energy dissipation. This situation would result in constant abiotic conditions that would favor the growth of a monospecific plant community.

5. Analysis of the new capping structure

5.1. Modification of the capping structure design

5.1.1. Description of the new design

A new design of the capping structure was produced by Tecsult following recommendations proposed after the first analysis of the local abiotic factors as presented in the first 3 chapters. These recommendations are briefly outlined in the next paragraph. This new is roughly similar in shape to the initial version (Figure 29 and 30). Differences can be summarized in few points : the slope of the edges are slightly steeper, the limit of the structure is partially emergent and the central part of the capping structure is in shallow water.

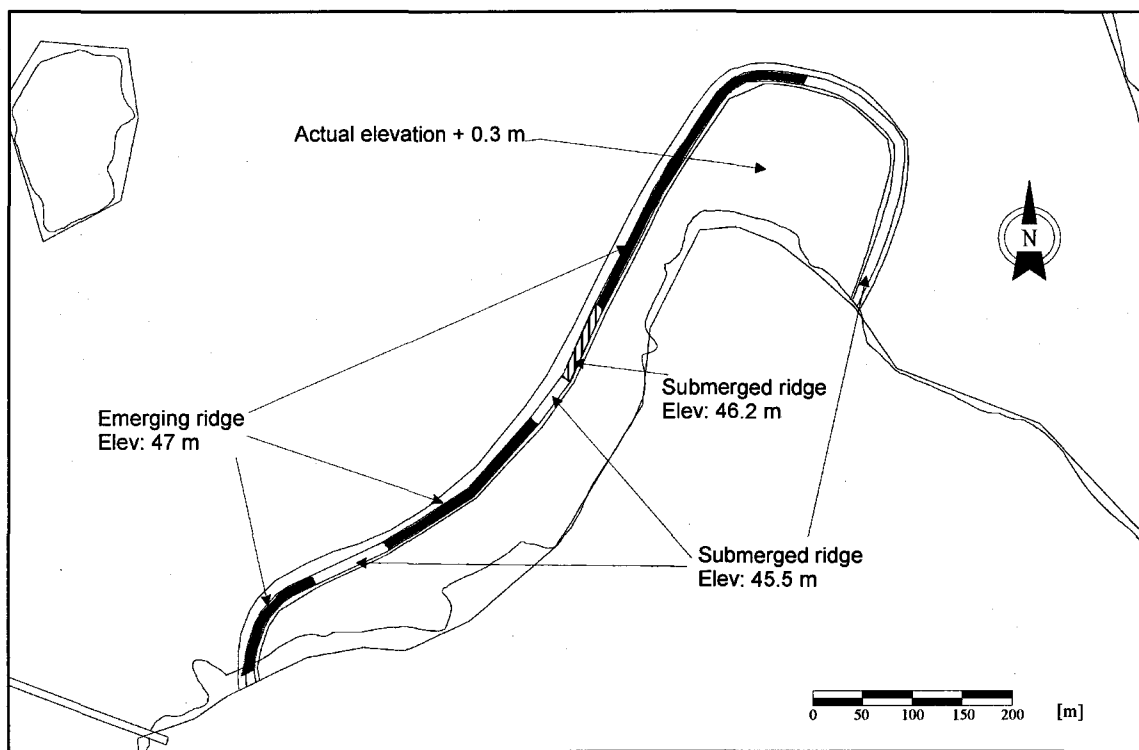


Figure 29 : Illustration of the new capping structure.

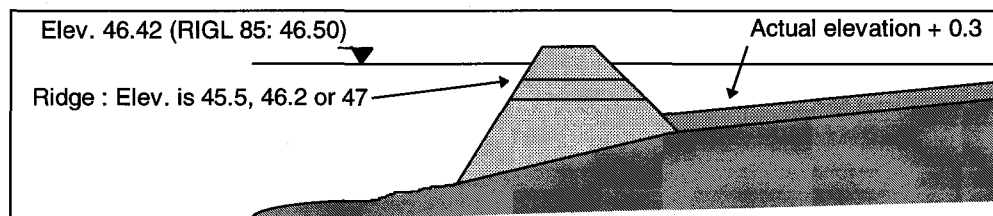


Figure 30 : Profile of the new capping structure.

5.1.2. Main advantages of the new design

This new design has several advantages in terms of habitat diversity and sustainability compared to the first one. The most important innovation of this new design is the creation of very diverse abiotic conditions concentrated in a relatively small area.

The presence of emergent « islands » around the structure will protect the internal part of the structure from ice-scouring, especially during the spring thaw. These emergent breakers can be used by several nesting bird species requiring protected and dry areas. Later, these islands will be naturally colonized by shrubs and trees. The occurrence of openings within the emergent structure will favor water circulation and diffusion of wave energy, creating diverse abiotic conditions : zones with relatively important wave energy and currents along with more quiet areas. In a long term perspective, wave energy is important in order to « clean » the structure from organic material, maintaining the potential for fish spawning on the substratum and eliminating the possibility for emergent plants to colonize the entire area, keeping an open water channel within the structure. This basin will favor a better circulation of water within the capping structure which will become a feeding area for fish and juvenile waterfowl.

As suggested earlier, habitat diversity induces species diversity : the new design creates a variety of abiotic conditions that will favor and maintain diversified habitats for plants and fauna. The first design would have resulted, because of the constant abiotic conditions, in a monospecific plant community.

5.2. Hydrodynamic modeling

5.2.1. Data

The new capping structure was integrated in the numerical field model (NMF) in order to replace the design of the first capping structure. The new elevations of the emergent ridge, the external and internal slopes of the structure and the amount of materials added in the central part of the structure were provided by Tecsult.

5.2.2. Modeling the hydrodynamics

Hydrodynamic simulations were produced with the new capping structure. Simulations were carried out using the HYDROSIM model presented previously in section 2.2.1. The same physical data described in section 2.1 was used along with the same finite element grid (refer to section 2.2.2). Therefore no calibration or validation of the model was necessary for the simulations that were made in this section.

The event chosen to analyze the impact of the new capping structure was the event of October 1st which has also been used to validate the hydrodynamic model. This event was chosen because of its high recurrence frequency and also because we already had a simulation of the hydrodynamics at this flow with the actual topography, which allowed us to easily analyze the impact of the capping structure on the local currents. These conditions are as follows: the discharge at the entrance of the flow domain (upstream boundary) is 8200 m³/s and the discharges at Coteau control structure 1 and 3 are respectively 350 m³/s and 200 m³/s. The water level at the entrance of the Beauharnois canal (downstream boundary) is 46.36 m - RIGL 55 (RIGL 85: 46.44 m).

5.2.3. Results of hydrodynamic modeling

Results of the hydrodynamic simulation for a discharge of 8200 m³/s with the new capping structure are illustrated by figures 31 to 34. Figure 31 shows water depth as calculated by the model. In general, depth within the structure is relatively shallow, deepest parts are located close to the ridge (figure 31). Note that a more precise topography is presented with wave modeling (Section 5.3). Velocities within the structure are very small less than 0,02 m/s (figure 32). Related shear velocities are also small within the structure and reach 0.008 m/s in the eastern part (figure 33). Figure 34 presents the difference of velocities between simulation with the new capping structure and present conditions. These differences are localized immediately around the new structure.

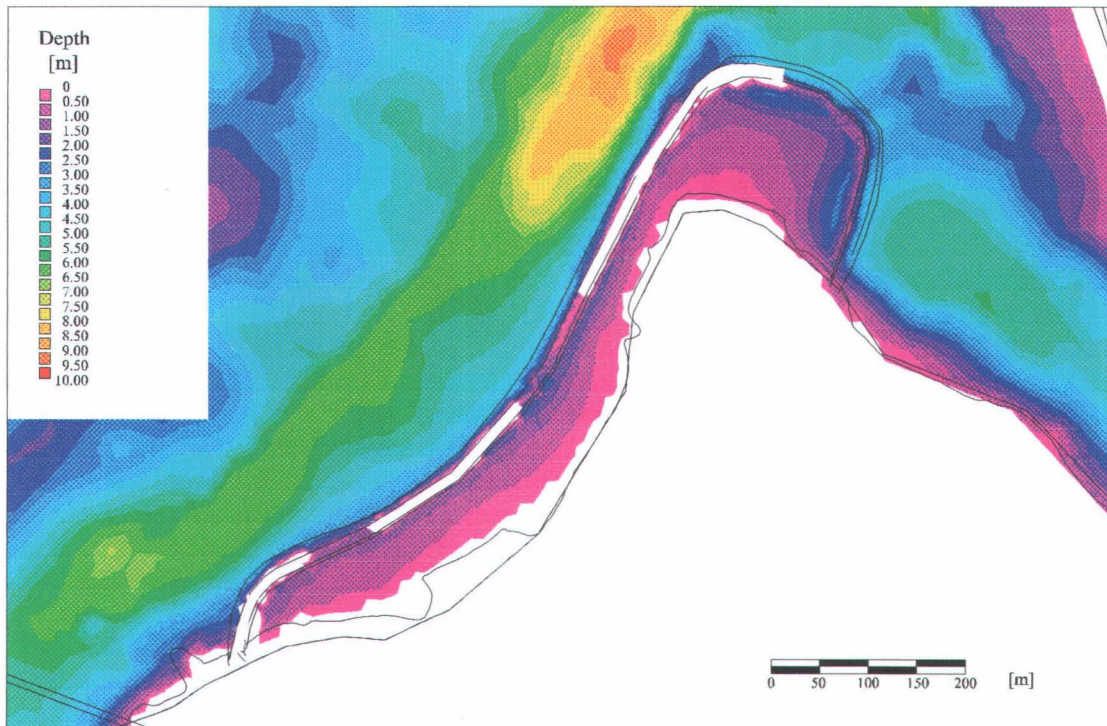


Figure 31 : Depth in the vicinity of Clark Island at a flow of 8 200 m³/s with the new capping structure.

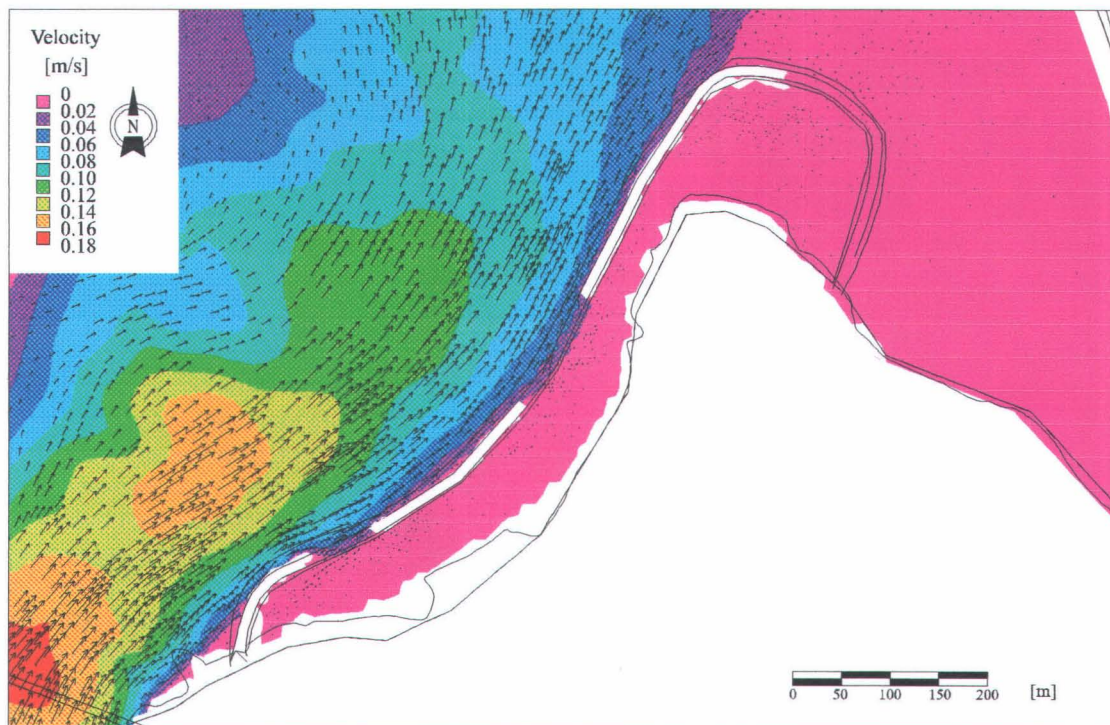


Figure 32 : Velocity in the vicinity of Clark Island at a flow of 8 200 m³/s with the new capping structure.

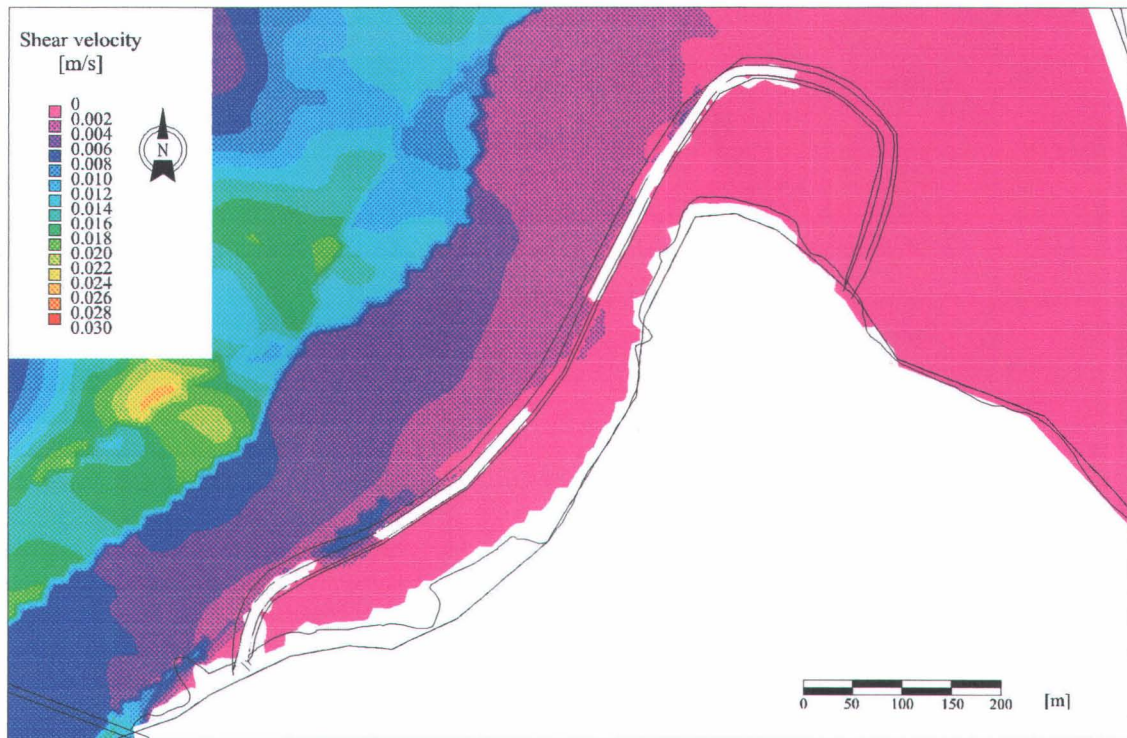


Figure 33 : Shear velocity in the vicinity of Clark Island at a flow of 8 200 m³/s with the new capping structure.

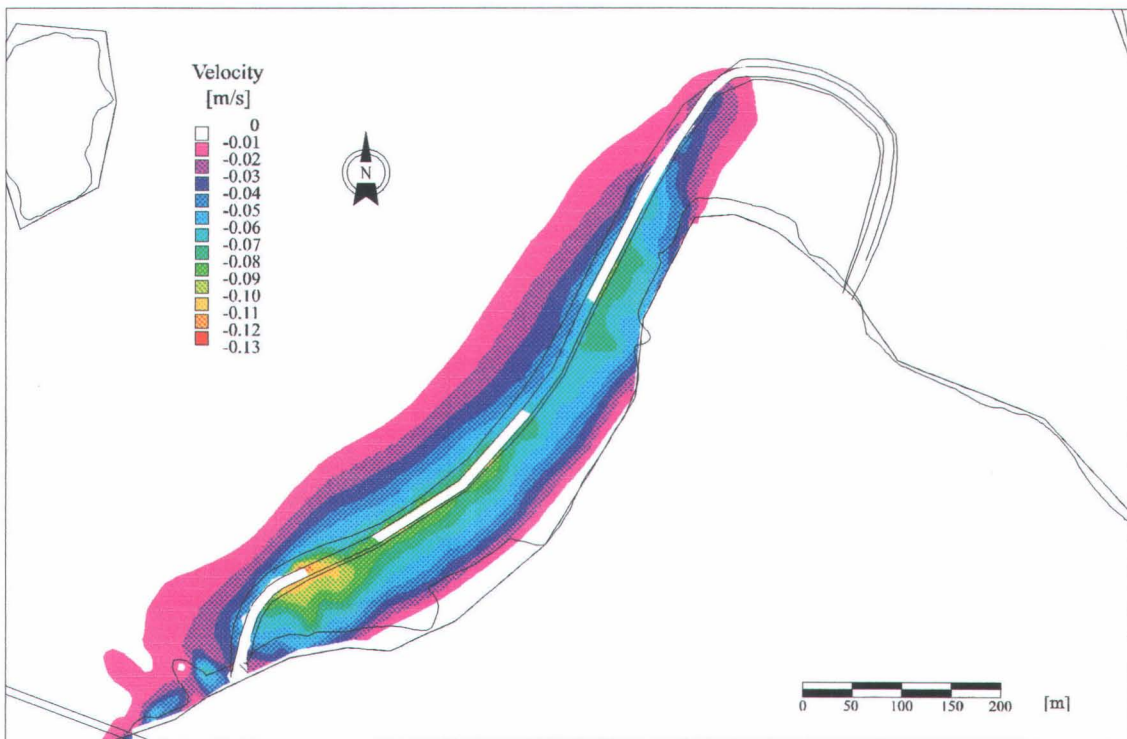


Figure 34 : Differences between velocities simulated with and without the new capping structure at a flow of 8200 m³/s.

5.3. Wave modeling

5.3.1. Data

Topographical description of the new capping structure (Numerical Field Model) was integrated to the wave model using the MODELEUR, with the same method used for hydrodynamic modeling.

Simulated events are exactly the same in terms of wind speed and direction as in the simulated event of Chapter 3. These wind directions (N-O, O, S-O) are typical of the area and their speed (60 km/h) represents relatively rare conditions. We believed that these conditions are « structuring » for plants, sediment and any other resisting material. Water level and current velocity introduced in the wave modeling were the same as in the event described in Chapter 3.

5.3.2. Modeling the waves

The wave model used is the HISWA model from Delft University (see Chapter 3). This model uses regular rectangular grid for calculation and for supporting the topographic data (figure 35), water level and currents. The simulations were performed using the same 25 m grid, containing 58 000 nodes, used in Chapter 3. However, because of the interpolation problem caused by the use of this type of grid when it is at an angle with the main structures, we had to refine a nesting grid over the capping structure that comprises 198 000 nodes with a mesh size of 2 m. Other conditions like directional sectors and spectral domain are the same as what was used in Chapter 3.

5.3.3. Result of wave modeling

The result of wave modeling is presented in figure 36. This figure is an integration of three simulations ; it is the maximum shear stress calculated by the model for each node of the domain in any of the three simulation results. A similar image of the area for the same wind conditions, but without the capping structure, is available in Chapter 3.

The distribution of wave energy is presented in figure 36. The maximum shear stress is located at the margin of the structure where it faces the main wave directions. Within the structure, the wave energy is relatively small, but three areas corresponding to the three openings in the structure have a relatively high shear stress of 0.4 to 0.6 m/s. In protected area, directly located behind emergent islands, wave energy and shear stress are minimum.

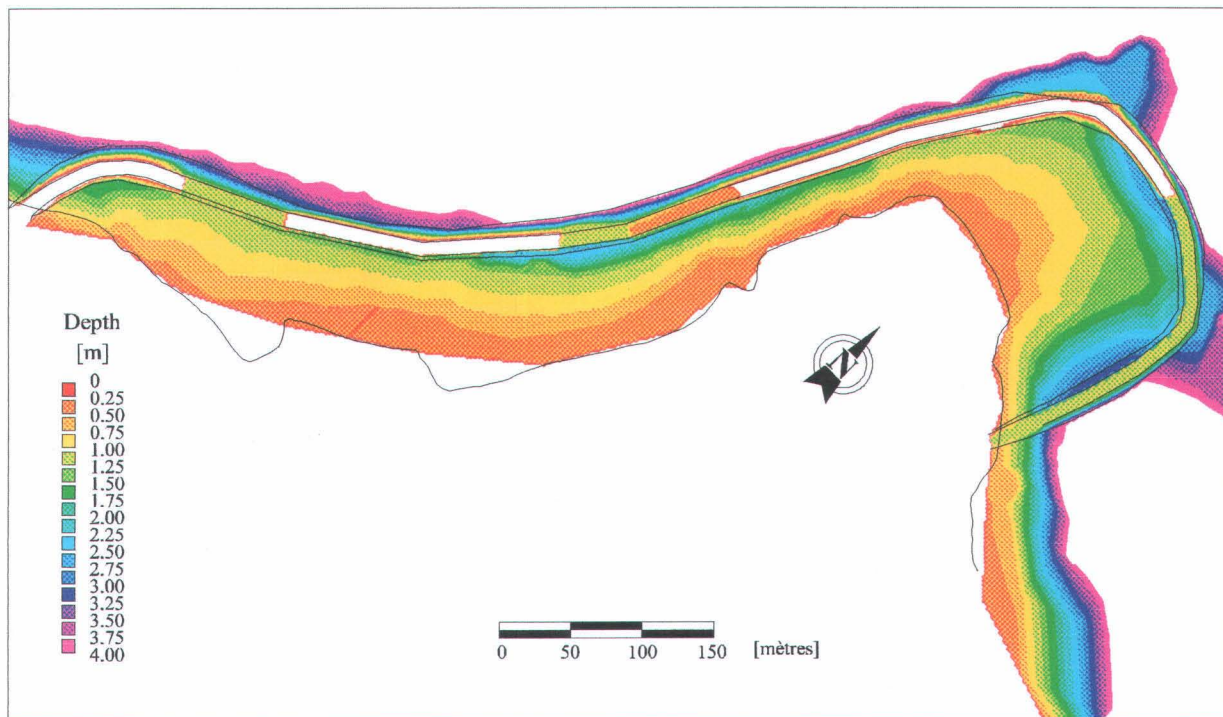


Figure 35 : Water depth within the capping structure as introduced in the wave model (created with 8 200 m³/s simulation).

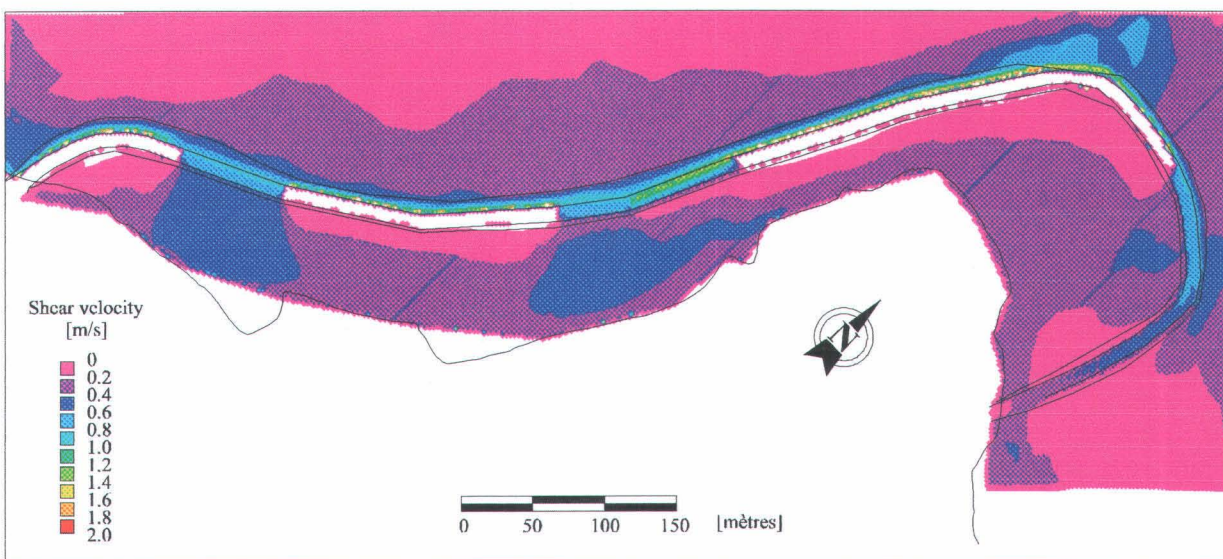


Figure 36: Wave induced shear velocities with the new capping structure.

5.4. Plant habitat modeling

5.4.1. Methodology

Plant habitat preferences were analyzed in Chapter 4 and the methodology used herein is the same as presented in that chapter. Briefly, this methodology uses the preference of each species of plants of interest for certain abiotic factors. These abiotic factors are the current, the substratum, the water depth and the wave shear stress. Once preferences for every factor is determined from species growing in the area, the modeling of these abiotic factors for the new structure allows to predict which plants will be growing better in a given area.

This structure is to be built and, as explained earlier, the type of substrate available for plants is not relevant because it is possible to plan its nutrient level and its physical properties. As modeled, current velocities are not discriminating for plant species in the sense that the range of speeds within the structure is suitable for all three selected plant species. Waves and water levels are the controlling factors for plant distribution within the planned structure.

5.4.2. Recommendation for revegetalization

Three species are particularly suitable for revegetalization (see Chapter 4 for justification). *Typha latifolia*, *Typha angustifolia* and *Scirpus lacustris* have different preferences in terms of abiotic factors (see Table 6). *Typha latifolia* prefers habitats in very shallow water with neither currents nor waves. *Typha angustifolia* lives in deeper water and supports relatively high wave energy. *Scirpus lacustris* has similar preferences but it is more resistant to waves and it was found growing in deeper water.

Using the wave shear stress and water depth distribution in the structure, we were able to propose a revegetalization plan based on habitat preferences of the three selected species. Figure 37 shows the proposed distribution of emergent plants within the structure. *Typha latifolia* is located in shallow (less than 40 cm) and protected areas. *Scirpus lacustris* is present in areas with water depth varying from 10 to 100 cm and shear stress ranging from 0.4 to 0.6 m/s. *Typha angustifolia* is present in approximately the same depth range, but in areas with less shear stress.

Fine organic rich material has to cover the areas that are selected for planting or seeding. We suggest that 30 cm of this material should be in place before planting or seeding. Even if the need for sediment thickness is slightly different for each species, 30 cm of material is suitable for all of them. *Scirpus lacustris* is more tolerant and should be considered first, if this material is rare and expensive : 10 cm appears to be sufficient.

5.4.3. Recommendations for structure amelioration

This structure design has the main advantage to put in close association various types of habitats. Emergent and submerged plants, fishes, water fowl, mammals and reptilians are certainly going to colonize the site. In order to maintain this system stable, it is important to maintain a good

water circulation within the structure, with currents and wave action. In order to keep an essential porosity in the gravel for fish spawning and habitat diversity, wave action has to be sufficient in a larger portion of the structure and water velocity is to be slightly increased. Evacuation of fine sediment is produced by a combination of wave action resuspending the material within the water column and currents transporting it outside of the structure.

Increasing the wave energy can be done by widening the apertures by several meters, mainly in the central part of the structure (Figure 38). Increasing the water velocity and therefore reducing the residence time can be done by slight modifications of the margin design. These modifications can be listed as follows : 1) reduction of the size of the western margin, 2) increase the size of central aperture, 3) increase water depth in a small portion of the eastern threshold to favor water exit. In order to avoid the filling by sediment and covering by aquatic plants of the central part we suggest to 4) slightly increase the distance of the emergent island in order to have a deeper channel and 5) cover the side of this « channel » with boulders, shaped in steep angles, so that it can be used as nursery for juvenile fishes. Plant growth in that area would considerably reduced water circulation within the structure.

These improvements would not change the hydrodynamic around the capping structure and would not change in a significant manner the hydrodynamic within the structure ; the only changes would be a slight increase of velocities (less than 1 cm/s) and a reduction of the residence time (renewal rate). Changes in the impact of wave action is also minor. The enlargement of aperture would not increase the shear stress within the structure but would extent the area where waves have a certain influence.

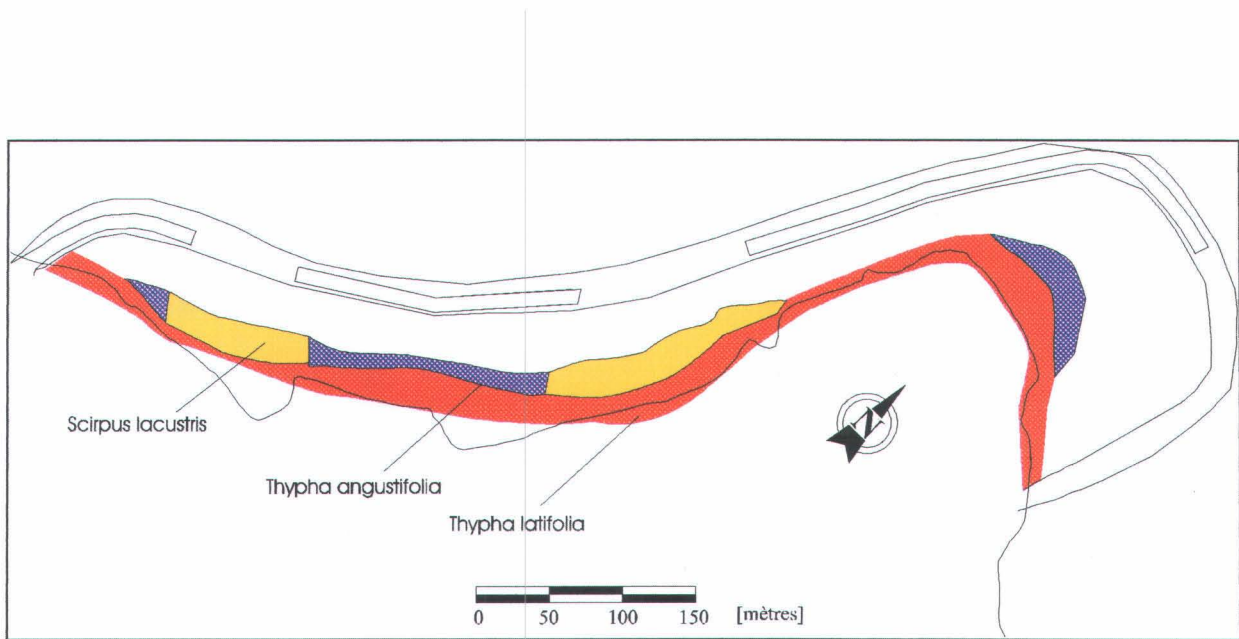


Figure 37: Recommendation for revegetalization.

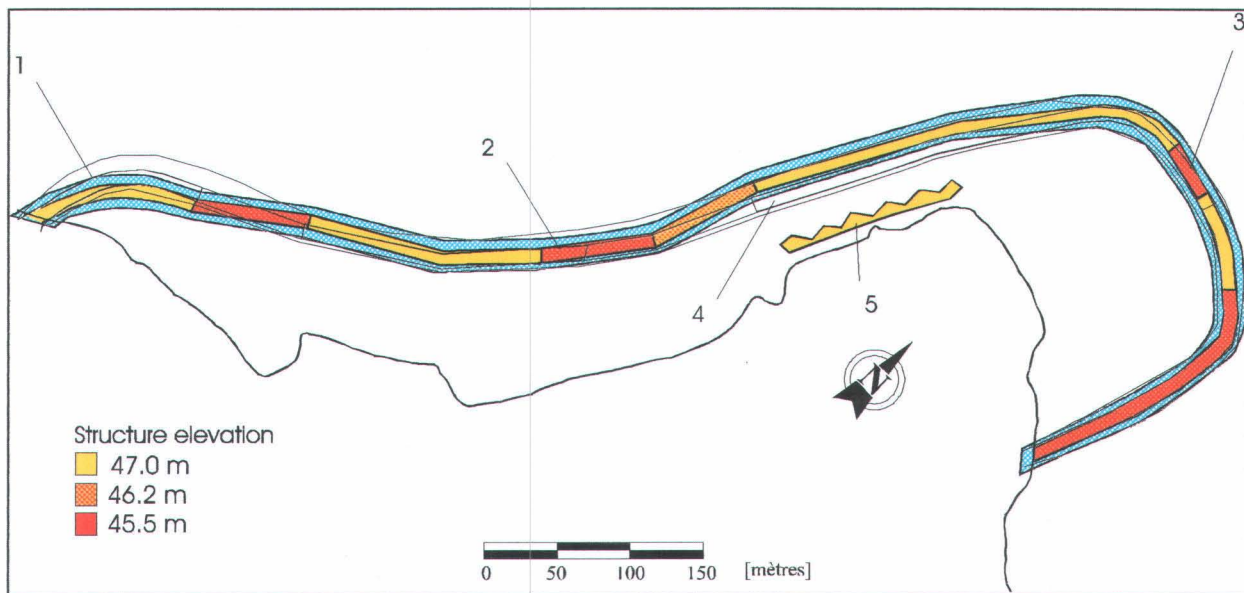


Figure 38: Recommendation for structure amelioration.

6. Conclusions

This report presents an original method of analysis for improving biodiversity on restored fluvial and lacustrine sites, that resulted in an original concept of intervention. This method integrates hydrodynamic, wave and plant habitat modeling, where hydrodynamic and wave models are used as incoming variables for modeling plant habitat. It was inspired from a microhabitat method : abiotic factors influence on selected emergent plant species were analyzed from natural setting and returned into proposed scenarios. We have analyzed in detail the impact of a capping structure on currents and waves and proposed a revegetalization plan using habitat preferences for emergent species. The analysis looked at two different structures : the first was covering the entire area and left 10 cm of water on the top of it, the second was proposed after suggestions for improvements from the first part of this report. The second structure clearly improved, used an original concept that favors a close association of divers habitat type. This new structure appears to be more diverse in terms of abiotic factors, therefore more efficient in terms of biodiversity.

The proposed capping structure was integrated in the Numerical Field Model (NFM) in order to simulate the hydrodynamics around the structure for different hydrological events. The water level and the velocities in the vicinity of Clark Island are influenced mostly by the discharge through the Coteau control structures. In general, current velocities around the structure are small and corresponding shear stress are not significant given the specifications of the proposed structure. Wave modeling performed with and without the capping structure suggests that wind energy is important in the study area. Significant erosion occurs at the site. The capping structure will concentrate waves and dissipate the wave energy mainly on the ridge. Waves are an important component of plant habitats ; simulated wave shear stress was used to establish plant habitat preferences. Several plant species are presently growing around Clark Island. *Typha angustifolia*, *Equisetum fluviatile*, *Scirpus lacustris*, *Carex aquatilis*, *Scirpus fluviatilis* and *Nymphaea* sp. are relatively abundant on the northeast side of the island. Emergent plants were characterized in terms of habitat preferences for substrate, current velocities, water depth, and wave exposure. These preferences set the limit of implantation of these species for the revegetalization of the structure. In the proposed scenario, wave-resistant *Scirpus lacustris* is planted in area with strongest wave energy facing apertures in the structure and the two species of *Typha* are planted over the rest of the capping structure according to water depth and wave energy. Reintroduction of these species (or others) is necessary in order to prevent invasion by exotic species like the aggressive Purple Loosestrife (*Lythrum salicaria*).

In order to insure the long term preservation of habitat diversity within the structure, we have suggested several improvements of the design that will maintain a suitable equilibrium between incoming sediment and organic matter production within the structure. The objective of these modifications is to improve water circulation and wave energy distribution within the structure.

7. References

- Auclair, A. N., Bouchard, A. et Pajaczkowski, J., 1973. Plant composition and species relations on the Huntingdon Marsh, Quebec. *Can. J. Bot.* 51 : 1231-1247.
- Booij, N., L.H. Holthuijsen, J. Dekker and Shoonbeek, 1993. Standard tests for the shallow water wave model HISWA version 100.21 Delft University of Technology, Department of Civil Engineering, Group of hydraulic and Geotechnical Engineering, 43 p.
- Boudreau, P., Morin, J. Secretan, Y., Leclerc, M., Drapeau, G., Chiasson, Y., 1995. Étude par modélisation hydrodynamique de solutions visant la restauration de la plage de la baie de la Faim, lac Saint-François. Pour Hydro-Québec. RP-437.
- Couillard, L et P. Grondin, 1986. La végétation des milieux humides du Québec. Les publications du Québec, Gouvernement du Québec, 400 p.
- Dodge, D. and R. Kavetsky. August 1995. Aquatic Habitat and Wetlands of the Great Lakes. SOLEC Working Paper presented at State of the Great Lakes Ecosystem Conference [online]. EPA 905-R-95-014. University Center, Mich. : Consortium for International Earth Science Information Network (CIRESIN).
- Heniche, M. Y. Secretan, P. Boudreau, and M. Leclerc. (1997) A new 2-D finite element drying-wetting model for rivers and estuaries. To submit at International Journal for numerical Methode in Fluids.
- Lorrain, S., Jarry, V., Guertin, K. 1993 Répartition spatiale et évolution temporelle des byphényles polychlorés et du mercure dans les sédiments du lac Saint-François; 1979-1989. Centre Saint-Laurent, Environnement Canada. 63 p.
- Fleurbec (auteur et éditeur), 1987. Plantes sauvages des lacs, rivières et tourbières, guide d'identification Fleurbec. Saint-Augustin (Portneuf), 400 p.
- Morin, J., Boudreau, P., Leclerc, M. 1994. Lac Saint-François : les bases de la modélisation hydrodynamique INRS-Eau No R-412. 67 p.
- Morin, J., Y. Secretan, P. Boudreau and M. Leclerc. 1996. Integrated two-dimensional macrophytes-hydrodynamic modeling : application to Lake Saint-François (Saint-Lawrence river, Quebec) Proceedings, 2nd international symposium on habitat hydraulics Ecohydraulics 200, Quebec City, June 1996.
- Secretan, Y., M. Leclerc, Y. Roy et collaborateurs multiples. 1996. Logiciel MODELEUR. Développé pour le compte du Fonds de recherche et de développement technologique en environnement (MEF) et HMS-Énergie inc.

Spence, D.N.H. , 1982. The zonation of plants in freshwater lakes. Adv. In Ecol. Res. 12 :35-125.

Weisner, S.E.B. 1991. Whithin-lake patterns in depth penetration of emergent vegetation. Freshwat. Biol., 26 :133-142.

Yamasaki.S., 1984. Role of plant aeration in zonation of *Zizana latifolia* and *Phragmites australis*. Aquatic Botany, 18 : 287-297.